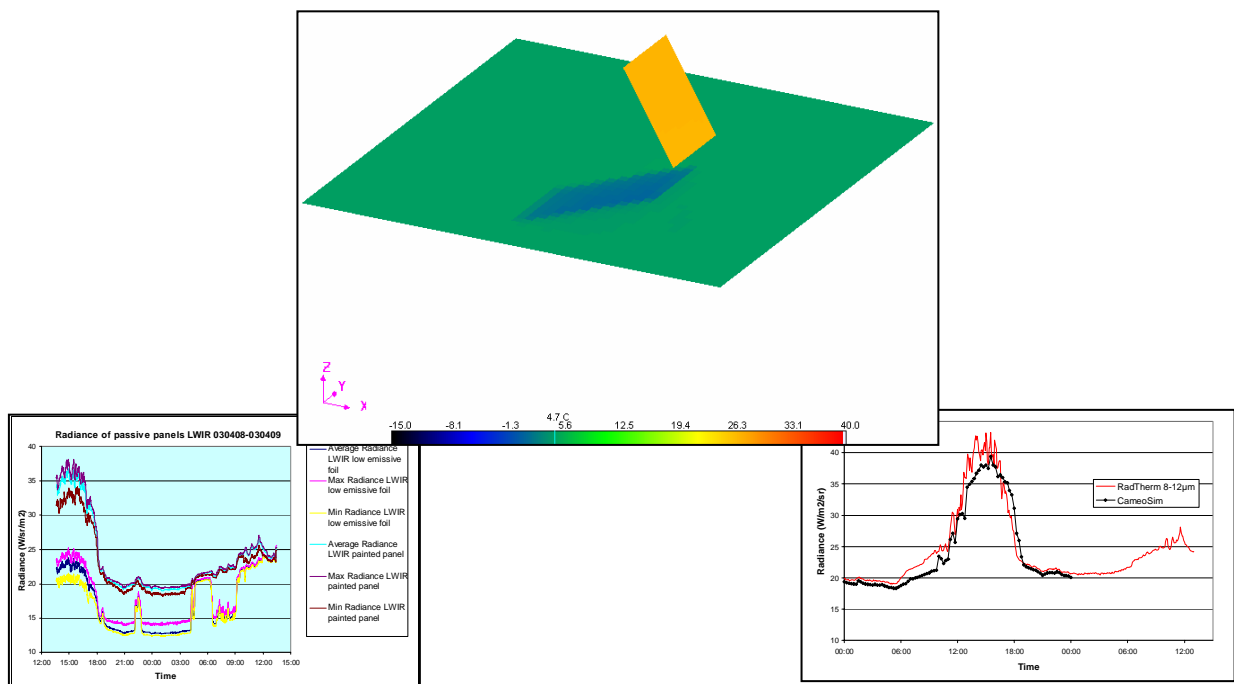


Patrik Hermansson, Annica Hjelm, Roland Lindell, Claes Nelsson, Andreas Persson, Stefan Sjökvist, Thomas Winzell

## Benchmarking and validation of IR signature programs: SensorVision, CameoSim and RadThermIR



SWEDISH DEFENCE RESEARCH AGENCY

Sensor Technology  
P.O. Box 1165  
SE-581 11 Linköping

FOI-R--0952--SE

September 2003

ISSN 1650-1942

**Technical report**

Patrik Hermansson, Annica Hjelm, Roland Lindell, Claes Nelsson, Andreas  
Persson, Stefan Sjökvist, Thomas Winzell

## Benchmarking and validation of IR signature programs: SensorVision, CameoSim and RadThermIR

<b>Issuing organization</b> FOI – Swedish Defence Research Agency Sensor Technology P.O. Box 1165 SE-581 11 Linköping	<b>Report number, ISRN</b> FOI-R--0952--SE	<b>Report type</b> Technical report
	<b>Research area code</b> 6. Electronic Warfare	
	<b>Month year</b> September 2003	<b>Project no.</b> E30163
	<b>Customers code</b> 5. Commissioned Research	
	<b>Sub area code</b> 62 Stealth Technology	
<b>Author/s (editor/s)</b> Patrik Hermansson                      Thomas Winzell Annica Hjelm Roland Lindell Claes Nelsson Andreas Persson Stefan Sjökvist	<b>Project manager</b> Claes Nelsson	
	<b>Approved by</b> Lars Bohman	
	<b>Sponsoring agency</b> Armed forces	
	<b>Scientifically and technically responsible</b>	
<b>Report title</b> Benchmarking and validation of IR signature programs: SensorVision, CameoSim and RadThermIR		
<b>Abstract (not more than 200 words)</b> <p>Computer programs for prediction of optical signatures of targets in background are valuable tools for several applications such as study of new platform concepts, new coatings, assessments of new sensor technology and development of tactics. This report covers a validation activity of three commercial optical signature prediction programs available at FOI: SensorVision, CameoSim and RadThermIR. As targets two flat panels with different emissivity was used, one close to unity and the other approximately 0.5. The panel signature was measured for a complete 24-hour period and radiance data for the panels were collected as well as supporting data consisting of weather data and contact temperature data.</p> <p>All three simulation programs were used to predict the radiance and the contact temperature of the panels. The simulation results were compared with the measurement results and they show considerable agreement. Some deviations were observed and they are analysed and discussed in the report. The largest deviations between measurements and modelling results are most likely related to weather parameters, such as windspeed, winddirection, cloudiness, etc. Generally, the low emissive panel was harder to predict than the paint panel, and MWIR was harder as compared to LWIR.</p> <p>The work gave valuable experience of the use of the programs.</p>		
<b>Keywords</b> CameoSim, IR, modelling, panel, RadThermIR, SensorVision, signature, simulation, Thermovision, validation		
<b>Further bibliographic information</b>	<b>Language</b> English	
<b>ISSN</b> 1650-1942	<b>Pages</b> 46 p.	
	<b>Price acc. to pricelist</b>	

<b>Utgivare</b> Totalförsvarets Forskningsinstitut - FOI Sensorteknik Box 1165 581 11 Linköping	<b>Rapportnummer, ISRN</b> FOI-R--0952--SE	<b>Klassificering</b> Teknisk rapport
	<b>Forskningsområde</b> 6. Telekrig	
	<b>Månad, år</b> September 2003	<b>Projektnummer</b> E30163
	<b>Verksamhetsgren</b> 5. Uppdragsfinansierad verksamhet	
	<b>Delområde</b> 62 Signaturanpassning	
<b>Författare/redaktör</b> Patrik Hermansson                      Thomas Winzell Annica Hjelm Roland Lindell Claes Nelsson Andreas Persson Stefan Sjökvist	<b>Projektledare</b> Claes Nelsson	
	<b>Godkänd av</b> Lars Bohman	
	<b>Uppdragsgivare/kundbeteckning</b> Försvarsmakten	
	<b>Tekniskt och/eller vetenskapligt ansvarig</b>	
<b>Rapportens titel (i översättning)</b> Benchmarking och validering av IR-signaturprogram: SensorVision, CameoSim och RadThermIR		
<b>Sammanfattning (högst 200 ord)</b> <p>Datorprogram för prediktion av optisk signatur hos mål i bakgrund är värdefulla verktyg för flera tillämpningar, t.ex. konceptstudier av nya plattformar, nya ytbeläggningar, värdering av ny sensorteknologi och taktikutveckling. Den här rapporten redovisar en validering av tre kommersiella program för prediktion av optisk signatur som finns vid FOI: SensorVision, CameoSim och RadThermIR. Som mål användes två plana paneler med olika emissivitet, den ena nära ett och den andra ca 0,5. Panelsignaturen mättes under en 24-timmarsperiod och radiansdata från panelerna registrerades så väl som kompletterande väder- och temperaturdata.</p> <p>Alla tre simuleringsprogrammen användes för att prediktera radiansen och kontakttemperaturen hos panelerna. Simuleringsresultaten jämfördes med mätresultaten och uppvisade stor överensstämmelse. Några avvikelser observerades och de analyseras och diskuteras i rapporten. Den största avvikelsen mellan mätningarna och simuleringarna är med största sannolikhet relaterade till väderparametrar såsom vindhastighet, vindriktning, molnighet, mm. Generellt sett var den lågemissiva panelen svårare att prediktera än färgpanelen och MWIR var svårare än LWIR.</p> <p>Arbetet gav värdefull erfarenhet av användningen av programmen.</p>		
<b>Nyckelord</b> CameoSim, IR, modellering, panel, RadThermIR, SensorVision, signatur, simulering, Thermovision, validering		
<b>Övriga bibliografiska uppgifter</b>	<b>Språk</b> Engelska	
<b>ISSN</b> 1650-1942	<b>Antal sidor:</b> 46 s.	
<b>Distribution enligt missiv</b>	<b>Pris:</b> Enligt prislista	

<b>1</b>	<b>INTRODUCTION .....</b>	<b>5</b>
<b>2</b>	<b>EXPERIMENTAL.....</b>	<b>6</b>
2.1	PANELS .....	6
2.2	AMBIENT AIR TEMPERATURE BLACKBODY REFERENCE .....	7
2.3	WEATHER STATION .....	7
2.4	THERMOVISION AND OTHER CAMERAS .....	8
2.5	MEASUREMENTS .....	9
2.6	RESULTS .....	10
2.6.1	Temperature images .....	10
2.6.2	Apparent radiance of the panels.....	13
2.6.3	Uncertainty analysis of Thermovision .....	16
2.6.4	Weather data.....	18
2.6.5	Contact temperatures .....	18
<b>3</b>	<b>SIMULATION SOFTWARE.....</b>	<b>20</b>
3.1	SENSORVISION .....	20
3.2	CAMEOSIM .....	21
3.3	RADTHERM IR .....	22
<b>4</b>	<b>CASE DEFINITIONS AND INPUT DATA.....</b>	<b>23</b>
<b>5</b>	<b>SIMULATIONS.....</b>	<b>23</b>
5.1	SENSORVISION .....	23
5.2	CAMEOSIM .....	25
5.3	RADTHERM IR .....	26
<b>6</b>	<b>RESULTS.....</b>	<b>27</b>
6.1	SENSORVISION .....	28
6.2	CAMEOSIM .....	30
6.3	RADTHERM IR .....	33
<b>7</b>	<b>DISCUSSION.....</b>	<b>38</b>
7.1	SENSORVISION .....	38
7.2	CAMEOSIM .....	38
7.3	RADTHERM IR AND COMPARISON WITH CAMEOSIM.....	39
<b>8</b>	<b>CONCLUSION .....</b>	<b>40</b>
<b>9</b>	<b>REFERENCES .....</b>	<b>41</b>
Appendix 1	Weather data from 8-9 April.....	43
Appendix 2	Weather data from 13-14 April.....	45

# 1 INTRODUCTION

Computer programs for prediction of optical signatures of targets in backgrounds are valuable tools in the process of designing different platforms and the study of new concepts with respect to stealth capability. In many cases it is necessary to treat the background in as much detail as the targets. There are other important reasons for the use of prediction programs, e.g. to improve the understanding of the signature processes; as a tool for assessment new sensor technology; for development of tactics; etc. All the applications raise different requirements on the signature prediction programs.

At FOI several commercial programs have been used for optical signature predictions. Some of them have been used for some time and others are more recently acquired. Validation of the programs is an important task that has to be fulfilled. The validation work is also an excellent way of improving the knowledge of the program and helps the development of efficient methods for the actual use of the programs. Many of the programs require huge amounts of input parameters and the work needed to properly assign values to these parameters should not be underestimated. Validation of commercial programs is of course being performed at other institutions, Ref 3, Ref 10 and Ref 15, and the work at FOI is to be seen as a complement to these previously reported validations. An earlier validation at FOI is reported in Ref 14.

This report covers a validation activity of three commercial optical signature prediction programs available at FOI: SensorVision, CameoSim and RadThermIR. SensorVision is a VEGA-based application that produces IR scenes in real time with a certain amount of simplifications in order to obtain the real time capacity. CameoSim is an advanced IR program aiming at producing high fidelity physics based images originally applied to camouflage assessments. RadThermIR is a 3-dimensional (with some restrictions) heat transfer program that uses Finite Difference Methods to predict the temperature distribution for a target and after that also predict the IR radiance. All three programs have their applications and they therefore complement each other. They are described in Chapter 3.

In this work simple targets are chosen and the background is treated in the simplest way like a flat plane. The targets consist of two panels with quite different surface emissivity, one is close to unity and the other is approximately 0.5. The panel signature is studied for a complete 24-hour period to emphasise the influence of a varying solar irradiance and sky cloud coverage. By using short time steps for the study, the dynamic behaviour can be monitored. The panels could be in either passive mode giving a panel temperature only dependent on the heat transfer from the surroundings, or in an active mode where the panels are heated internally simulating a real vehicle case for instance.

For the validation a new set of measurement data was collected for both of the panels and for both the passive and active case. At the experiment both radiance data for the panels were collected as well as supporting data consisting of weather data and contact temperature data. In this report the measurement results are presented together with an uncertainty analysis.

This report only shows predictions and validations for the passive case. RadThermIR could predict the active case whereas SensorVision and CameoSim do not have that capability. FOI

has previously showed how RadTherm can be used for improving the target signature modelling of SensorVision, see Ref 6. Validations for the active case are planned for the future.

Swedish normal time (not daylight-saving time) is used consistently through the report.

## 2 EXPERIMENTAL

### 2.1 PANELS

The purpose of the panels are to provide simple targets to study fundamental signature effects. The panels consist of different layers that form a flat surface of  $1 \times 1.2 \text{ m}^2$ . Thereby, the heat conduction problem becomes essentially one-dimensional. The surface scattering is also simplified since no internal reflections can occur between different parts of the target. One of the layers in the panel is a heat-foil to obtain higher temperatures of the panels. The foil is powered from a temperature controller. At the back of the panels there is a comparatively thick layer of insulating PVC foam, Divinycell, to minimize the heat flow through the back side of the panel. This decreases the power consumption when heating the panels and simplifies the heat conduction problem. The layers are attached to each other, either by glue or by two-face tape. A cross-section of the panels is shown in Figure 1. The panels were built by Saab Barracuda AB.

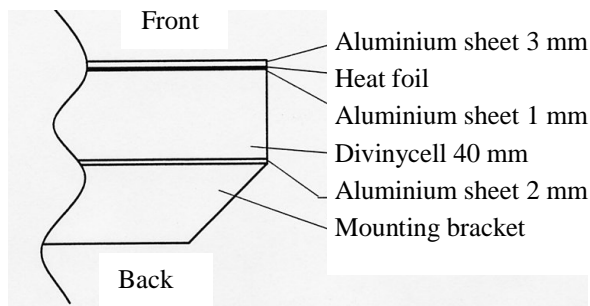


**Figure 1 Cross section of the panels.**

The two panels used for this experiment were coated differently. One of them was painted with standard Swedish dark green camouflage paint. The other one had a low emissive foil attached to the front surface with two face tape. The foil was also dark green but with a slight difference in colour compared to the paint.

The panels were mounted on stands of Aluminium, see Figure 2. The panels can be tilted from horizontal to vertical and further on 30 degrees to provide a negative angle. The angle is fixed by tightening large friction screws.



**Figure 2** The two dark green panels on stands: painted (left) and low emissive foil (right).

On each panel there was a Pt 100 temperature sensor mounted inside the front Aluminium sheet, close to the front surface. The sensor has a 4-wire connection to a chassis connector in a box on the back of the panel to enable monitoring and logging of the panel temperature. A second Pt 100 sensor is mounted in the same way and is used for the temperature controller for the heat foil. The Pt100 sensors were calibrated in lab and the result is shown in Table 1. The uncertainty was estimated to be 0.04 °C ( $k=2 \approx 95\%$  confidence level).

**Table 1** Calibration of Pt100 contact probes of the panels

Panel	Correction	Comment
Dark green paint	-0.06 °C	
Dark green foil	+0.17 °C	
Light green paint	-0.07 °C	Not used for this report

$$T_{\text{corr}} = T_{\text{meas}} + \text{Correction}$$

The temperature probes were connected to a logger AAC-2 which had an estimated uncertainty of approximately 0.1 °C ( $k=2 \approx 95\%$  confidence level).

## 2.2 AMBIENT AIR TEMPERATURE BLACKBODY REFERENCE

The ambient air temperature blackbody reference is a field blackbody consisting of a conical cavity. A fan ensures that the reference adapts to air temperature. The reference is further described in Ref 9. The reference has a Pt100 sensor installed to enable monitoring of the temperature. The readings of the sensor were corrected:  $T_{\text{corr}} = T_{\text{meas}} - 0.23$ . The temperature was logged on the same logger as the panels.

## 2.3 WEATHER STATION

The weather station was a Vaisala Milos 500, equipped with different kinds of weather sensors, see Table 2. Values were recorded every minute during the measurements. The weather station was placed in close proximity to the panels and started logging 24 h before the radiance measurements started. The weather station is shown in Figure 3.



**Table 2 Weather station parameters and sensors**

Weather parameter	Unit	Sensor specification	Comments
Wind direction	degrees	Vaisala WAV15A	
Wind speed	m/s	Vaisala WAA15A	
Air temperature	°C	Vaisala HMP45D	
Relative air humidity	%	Vaisala HMP45D	
Air pressure	hPa	Vaisala PTB200A	
Visibility	km	Vaisala FD12P	
Extinction coefficient	km <sup>-1</sup>	Vaisala FD12P	
Precipitation	ON/OFF	Vaisala DRD11A	
Type of precipitation	Rain/snow	Vaisala FD12P	
Intensity of precipitation	mm/h	Vaisala FD12P	
Rain accumulation	mm	Vaisala FD12P	
Snow accumulation	mm	Vaisala FD12P	
Present weather	NWS codes	Vaisala FD12P	
Global radiation ( 0.3 - 2.8 $\mu\text{m}$ )	W/m <sup>2</sup>	Kipp & Zonen CM 7B	
Reflected radiation ( 0.3 - 2.8 $\mu\text{m}$ )	W/m <sup>2</sup>	Kipp & Zonen CM 7B	
Sky radiation ( 3.5 – 40 $\mu\text{m}$ )	W/m <sup>2</sup>	Eplab PIR.	Had a temperature dependent offset during the measurement
Ground radiation ( 3.5 – 40 $\mu\text{m}$ )	W/m <sup>2</sup>	Eplab PIR	Did not work during measurement

**Figure 3 The weather station close to the panels and sensors.**

## 2.4 THERMOVISION AND OTHER CAMERAS

Two THV900 cameras were used, one long wave (LWIR) with filter LPL (7.5-12 $\mu\text{m}$ ) and one mid wave (MWIR) with filter Y02 (3.5-5 $\mu\text{m}$ ). The spectral response for the camera systems are shown in Figure 4. The cameras use a scanning technique with one detector and can therefore be radiometrically calibrated, with a result of 272x136 pixels at 15 Hz. The field-of-view of the camera lenses were 20°. The serial numbers of the Thermovision system used were 966001 for the MWIR and 976017 for the LWIR. The system was traceably calibrated before

the measurements, in June 2002. More information on the Thermovision system is found in Ref 9.

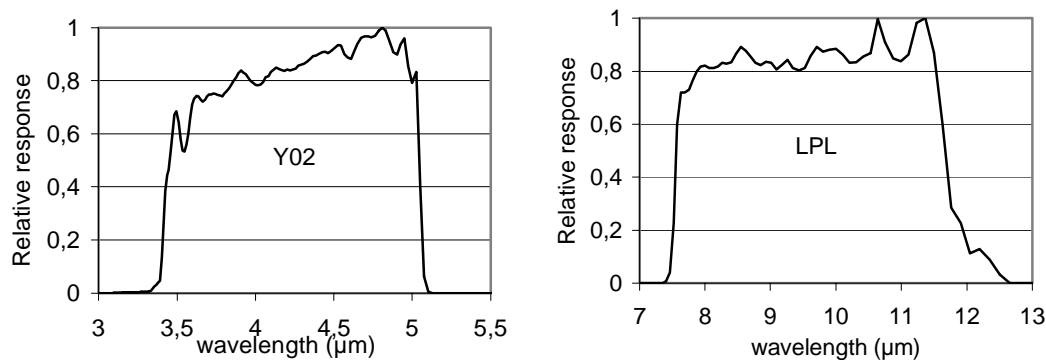


**Figure 4 Spectral responses of the MWIR (Y02) and LWIR (LPL) Thermovision cameras. At the same moment as an IR-picture was grabbed, also pictures were grabbed for each of the spectral bands: UV, NIR and visual. The visual band was covered by a RGB camera. All data was stored on hard disks directly.**

The cameras were mounted on a tripod and the controlling electronics and storage devices were placed in a van. As weather protection the tripod was covered with a plastic tarpaulin. The camera set up is shown in Figure 5.



**Figure 5 Camera set-up**

## 2.5 MEASUREMENTS

The measurements took place at the FOI site in Linköping. The panels and sensors were placed on a bank covered with grass. An overview of the set-up is shown in Figure 6. The position of the sensors was determined, by a handheld GPS navigator, to be N 58° 23.505; E 15° 34.537; elevation 73 m. The sensors were looking horizontally at the panels in a direction of 76° relative to north. The panels were placed 17.6 m from the sensors and the surface normals of the panels had a direction of 256° relative to north and an elevation of +30°.



**Figure 6 An overview of the measurement set-up. From left: weather station, sensors, panels and ambient air temperature reference.**

The measurements were made at two different occasions, 8-9 April and 13-14 April. The measurements continued for a 24-hour period at both occasions. The first was performed with passive panels and the second with active (heated) panels. To be able to correctly simulate the case with heated panels we used a power gauge to continuously monitor the input electric power.

After the measurements the IR-pictures were calibrated to yield the radiance according to the filter and detector combination used. The Matlab-based evaluation software IR-Eval was used to do this. The radiance was corrected for atmospheric transmission losses, which gave the radiance at the panel surfaces. The transmission was estimated with Modtran and turned out, as expected, to be practically negligible, see Table 3.

**Table 3 Estimated atmospheric transmission for the measurements.**

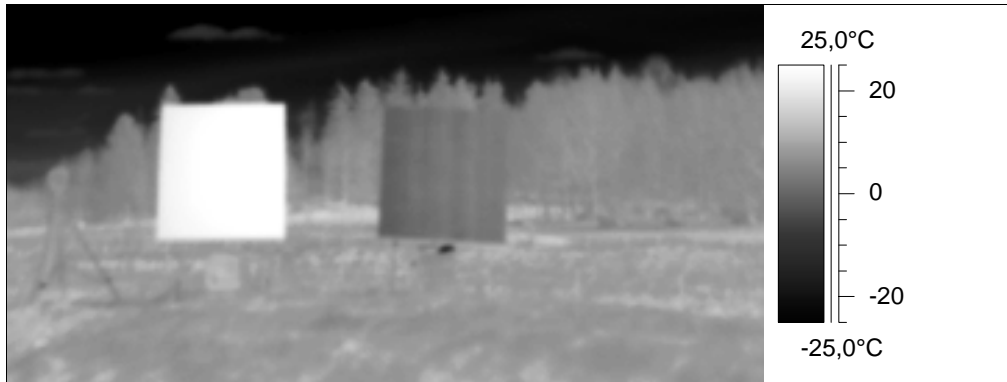
Band	2003-04-08	2003-04-13
LPL	99.57%	98.94%
Y02	99.13%	98.08%

A representative radiance value was calculated by setting out a polygon covering almost all of the panel front surface. Only a small part of the edge was omitted. The average, as well as maximum and minimum, radiance of each picture was calculated. This was done for all the images to create radiance series for comparison with the simulation results.

## 2.6 RESULTS

### 2.6.1 Temperature images

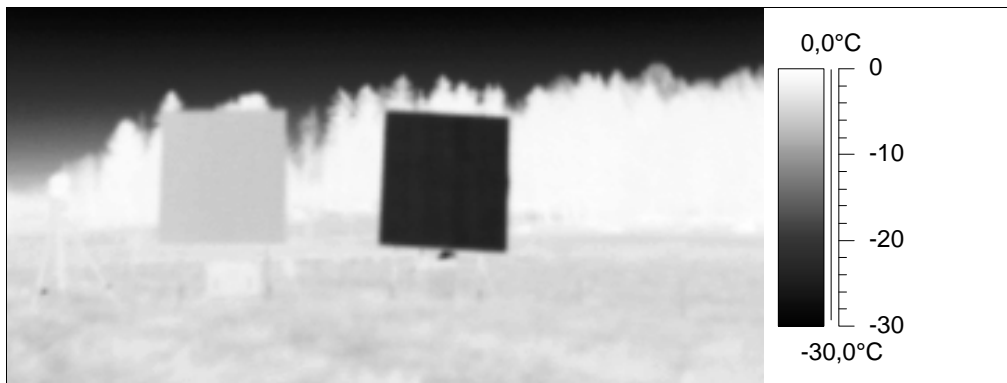
The temperature images show the apparent temperature in the images and are a good way of illustrating different phenomena. In Figure 7 and Figure 8 are some examples of images of the panels in passive and active mode. The images show how the contrast between the panels and the background varies with waveband, time, surface material and heating. The heating of the panels is done in four separate regions (as can be seen in Figure 8) which give a temperature drop between them. This results in a quite low minimum radiance for the active case. As can be seen on especially the last pictures, the heat influenced the adhesion of the tape. This resulted in detachment of the foil and a lot of large bubbles with lower temperature.



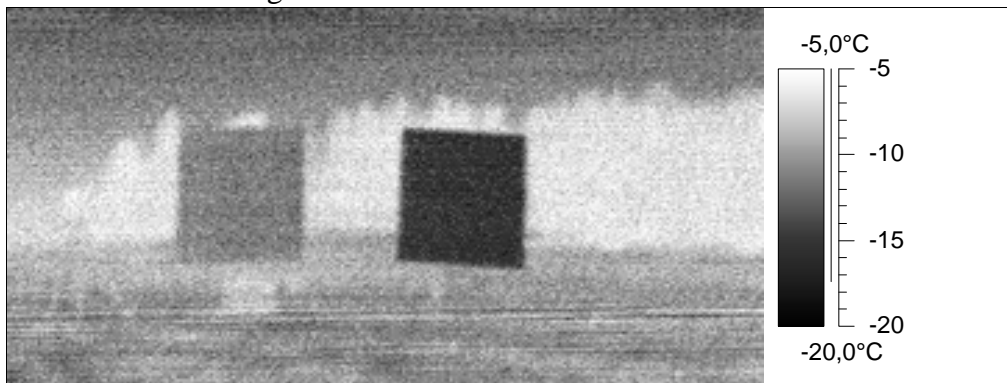
13:37:13 8/4 2003 Longwave



13:37:13 8/4 2003 Midwave



01:01:22 9/4 Longwave



01:01:22 9/4 Midwave

**Figure 7** Temperature images of the passive panels (not heated) for day and night time. Paint panel to the left and foil panel to the right. Please notice the different temperature scales.



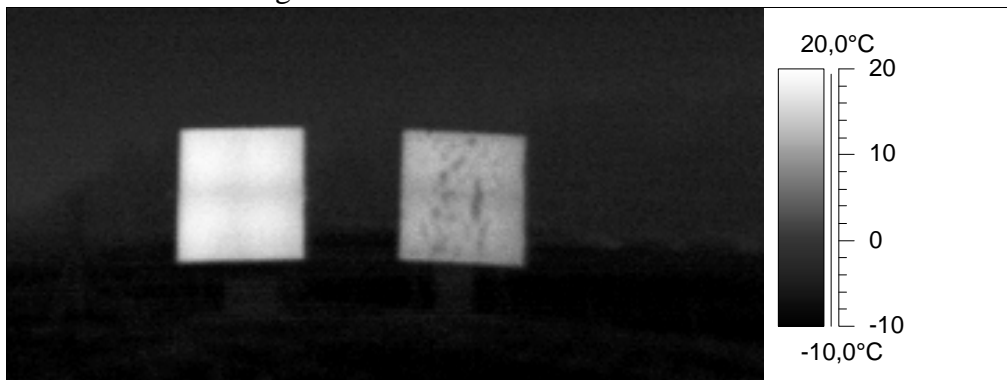
13:00:54 13/4 Longwave



13:00:54 13/4 Midwave



01:00:54 14/4 Longwave



01:00:54 14/4 Midwave

**Figure 8** Temperature images of the active panels (heated) for day and nighttime. Paint panel to the left and foil panel to the right. The large bubbles in the foil can easily be seen (right panel). Please note the different temperature scales.

### 2.6.2 Apparent radiance of the panels

The determined calibrated apparent radiance values of the panels are shown in Figure 9 for the passive case and in Figure 10 for the active case. These are the measurement results that later on are used for validation of the IR programs. The variations with the time of day are very obvious. It is also clearly shown how the sun irradiance differences between 8 April (sunny) and 9 April (cloudy) affects the radiance of the panels. The foil panel radiance makes dramatic shifts in radiance during the night which most probably is an effect of changing cloudiness. This was confirmed by the long wave sky irradiance measurement that was made with the weather station.

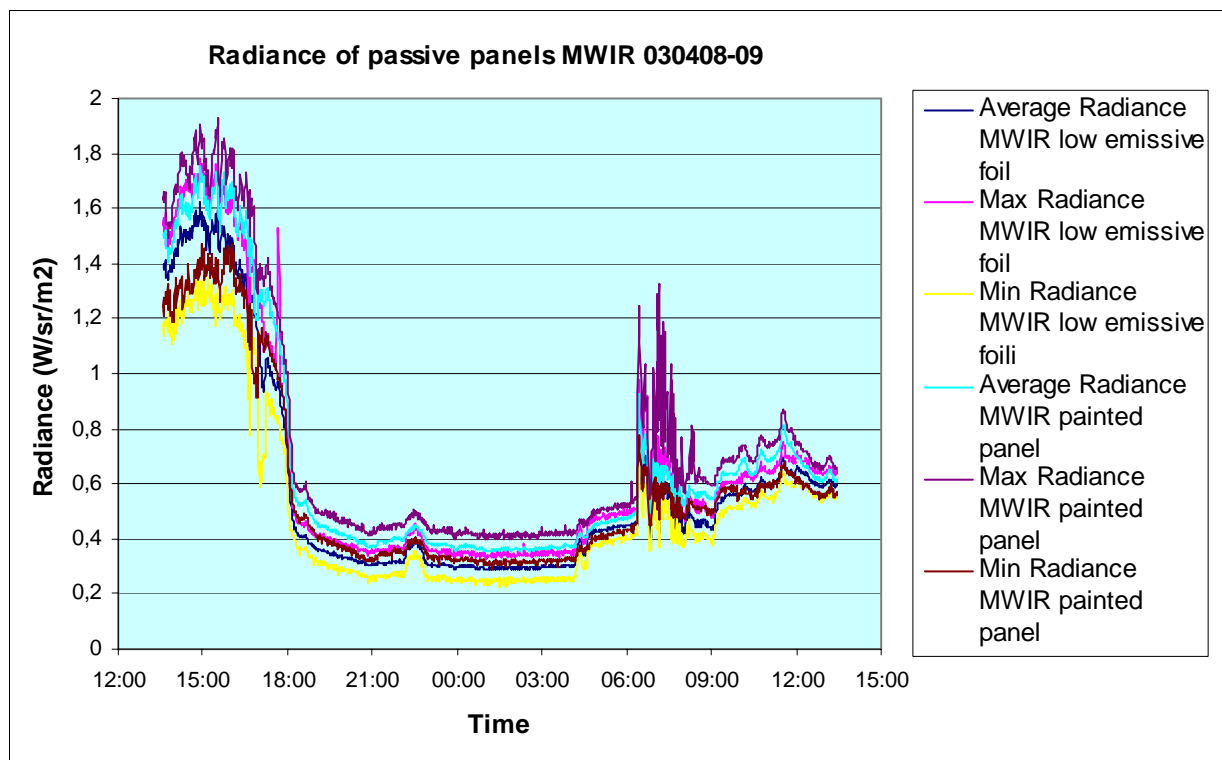
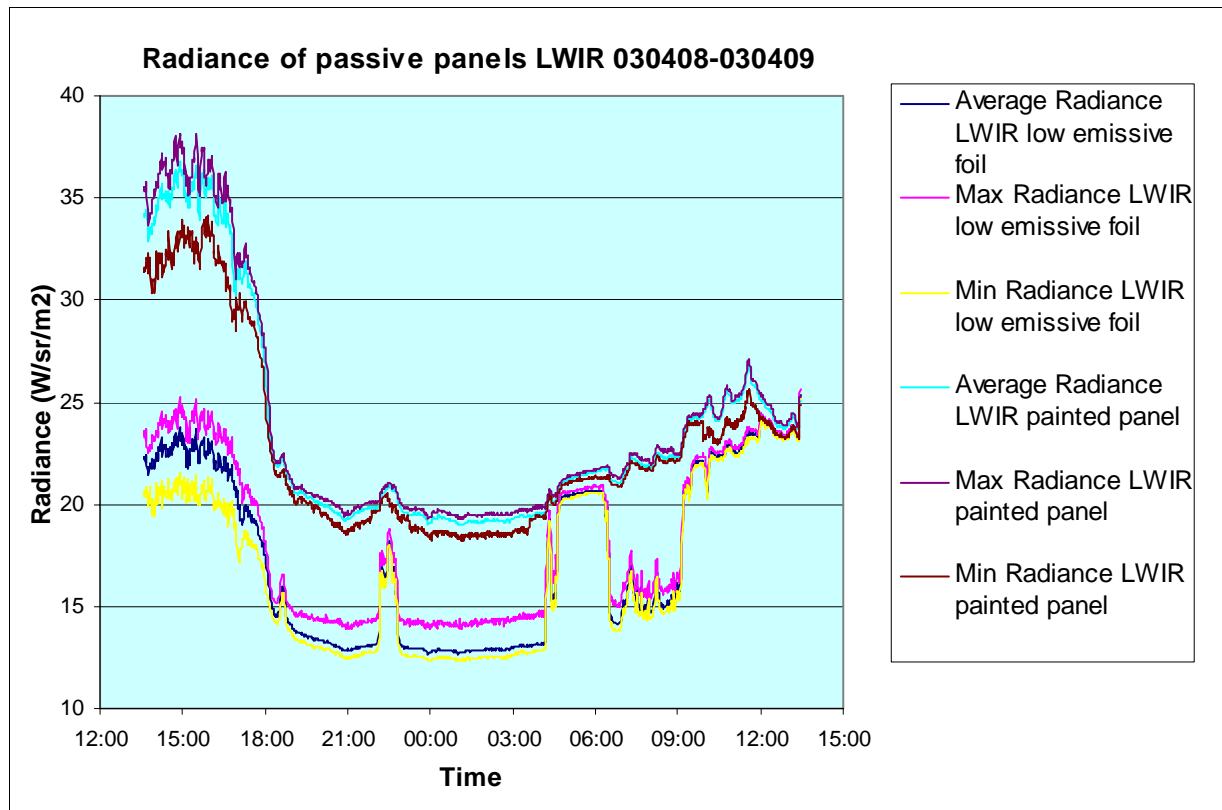


**Figure 9 Radiance as a function of time for the passive panels.**

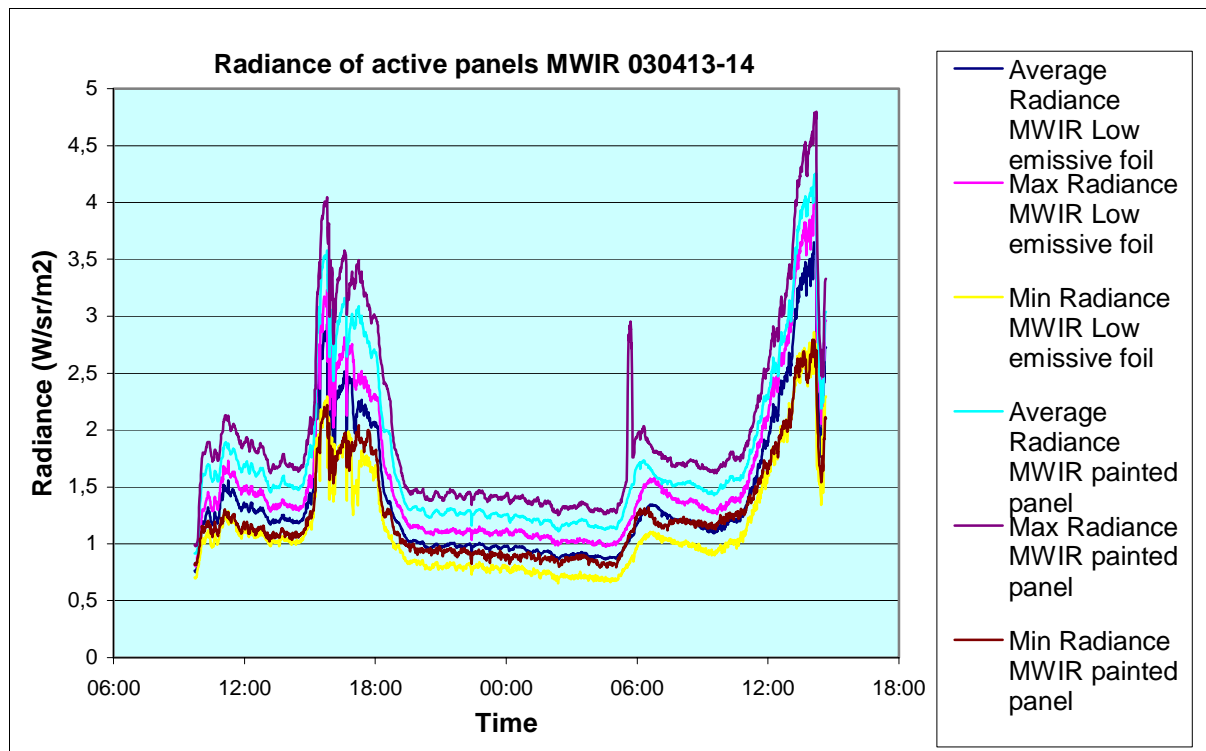
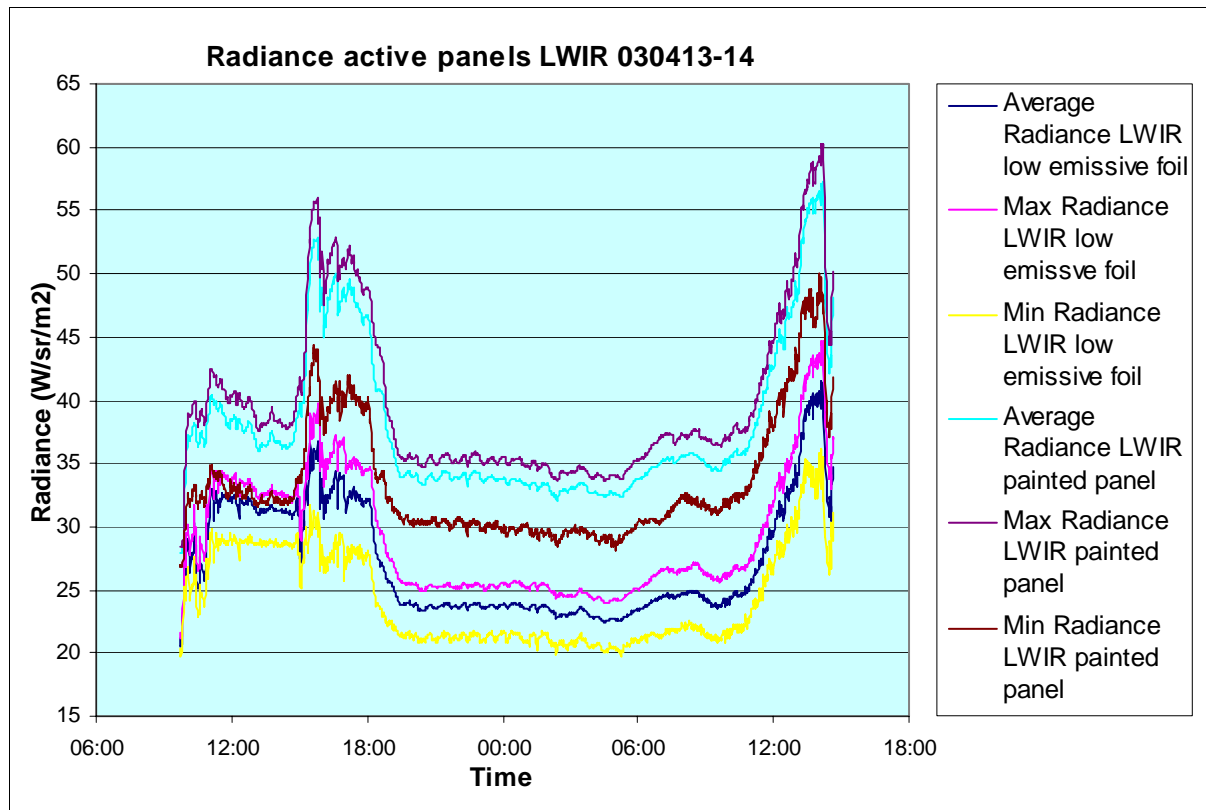


**Figure 10 Radiance as a function of time for the heated panels.**



### 2.6.3 Uncertainty analysis of Thermovision

In order to determine the uncertainty of the radiance measurements and the following data processing, comparisons were made between contact temperature measurements and Thermovision results for the ambient air temperature reference. The measured contact temperature of the ambient air temperature reference was used to calculate the blackbody radiance for the two Thermovision wavebands LPL and Y02. The result is shown in Figure 11 and Figure 12 where also the difference between the two methods is displayed.

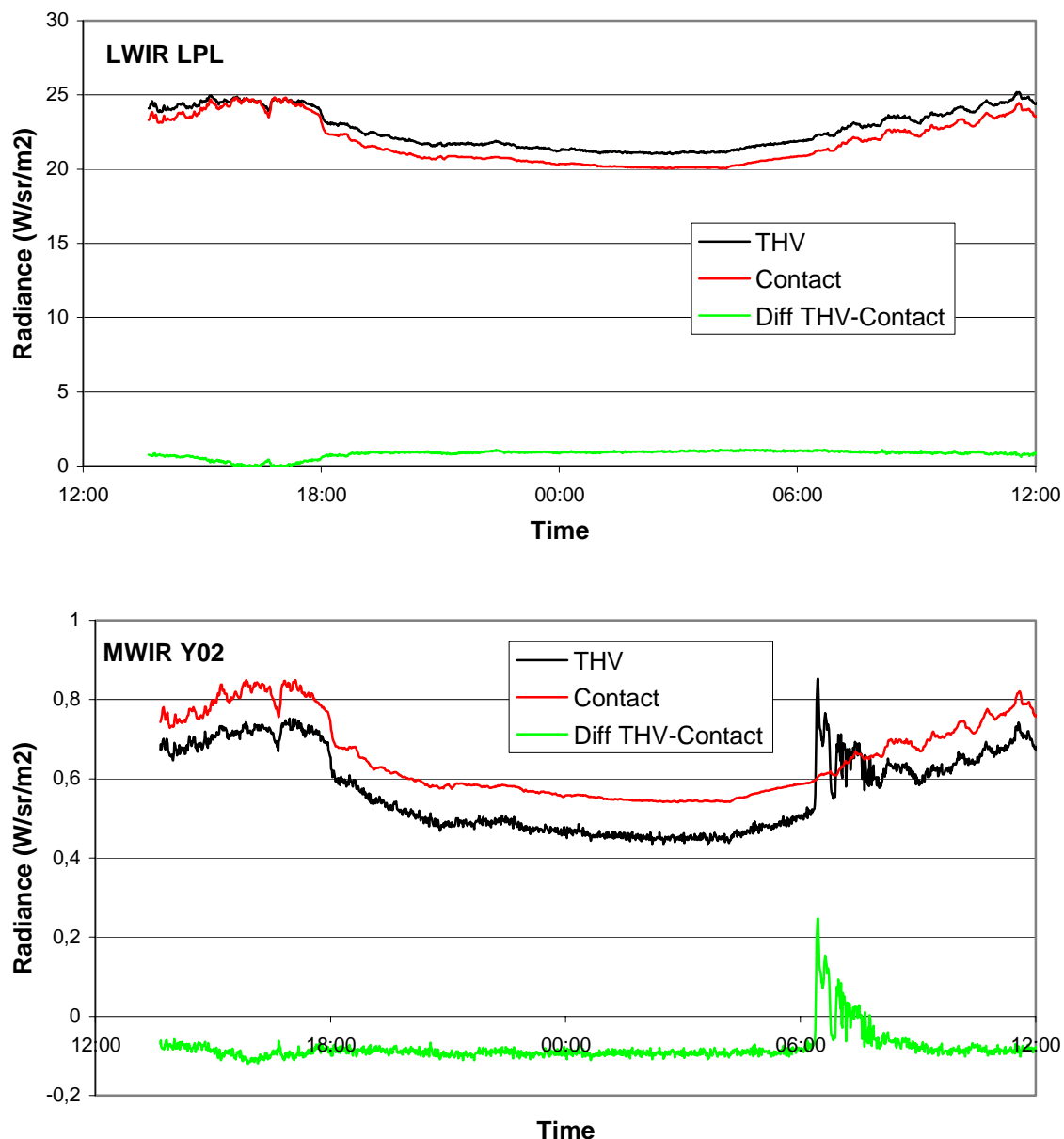


**Figure 11 Comparison of calculated blackbody radiance and the measured radiance of the ambient air temperature reference for the two wave bands, LPL and Y02. Results form the period of 8-9 April.**

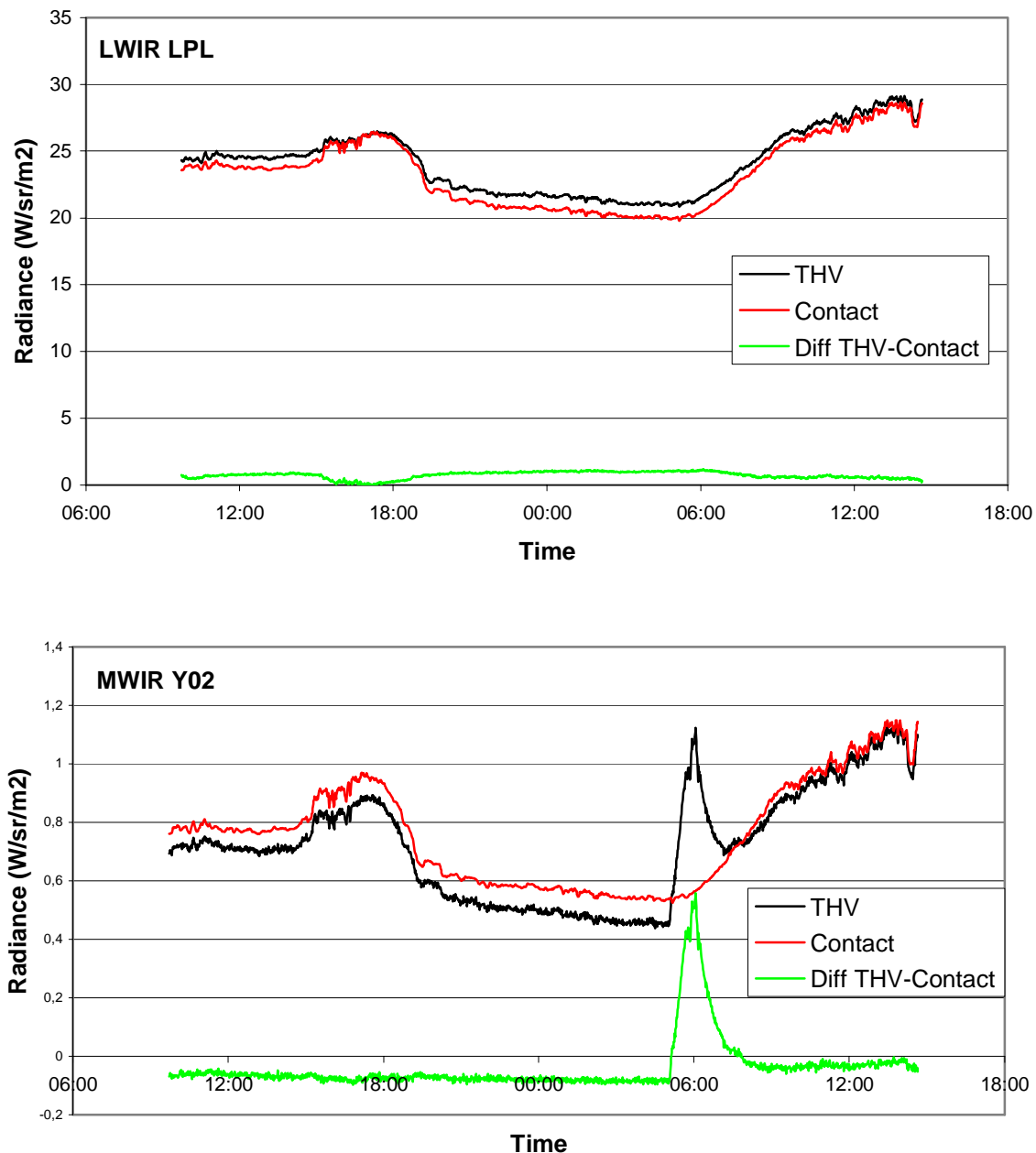


**Figure 12 Comparison of calculated blackbody radiance and the measured radiance of the ambient temperature reference for the two wave bands, LPL and Y02. Results from the period of 13-14 April.**

As seen in Figure 11 and Figure 12, there is a quite systematic difference between the measured and calculated blackbody radiance. If there were calibration errors in the Thermovision system they would probably manifest themselves as a radiance offset. The behaviour is very similar for the two measurement periods. During night time the heat fluxes in a scene generally are lower since there is no sun. The difference shown in Figure 11 and Figure 12 is also quite stable for the night and representative mean deviations can be calculated, see Table 4. The mean values are calculated for the period 7 pm to 5 am.

There are a few exceptions from the systematic difference but there are possible reasons for these. It is more likely that there actually were calibration offsets in the Thermovision system. During the afternoon of 8 and 13 April there is no difference between the radiance calculated

from the contact temperature and the measured radiance. At this time, it was very sunny and there was incident sun light on the ambient air temperature reference. This probably introduced an uncertainty of both the contact temperature measurement and the radiance measurement. The other exception occurs early in the morning when the sun elevation is very low. Probably this introduces stray light in the Thermovision lenses. This effect is seen in most of the data from the whole experiment. The conclusion is that it most probably was a constant offset in all Thermovision results and the size of this error is found in Table 4. The reader should bear these offsets in mind when studying the deviations between simulations and measurements in later chapters of this report.

**Table 4 Average difference between radiance from contact temperature measurements and from Thermovision.**

	<b>LPL</b>	<b>Y02</b>
	W/(sr m <sup>2</sup> )	W/(sr m <sup>2</sup> )
8-9 April	0.97	-0.091
13-14 April	0.96	-0.079

$$\text{Diff} = L_{\text{THV}} - L_{\text{calculated}}$$

The reliability of the calculated offsets depends on the accuracy of the calculated blackbody radiance of the reference. The uncertainty of the temperature logging system is estimated to be lower than 0.1 °C and lower than 0.04 °C for the temperature probes. The emissivity of the cavity of the ambient air temperature reference is estimated to be higher than 0.99. Since the temperature of the reference was very close to the air temperature it was reasonable to consider it a perfect blackbody, at least during night time. The conclusion is that the uncertainty of the calculated radiance for the spectral band LPL was in the order of 0.1 W/(sr m<sup>2</sup>) and for Y02 0.006 W/(sr m<sup>2</sup>). The calculated offsets are well above that.

A similar difference analysis was made with the processing software Thermacam Researcher provided by FLIR systems. The difference between measured apparent temperature and the contact temperature was determined to be about +2.5 °C for LPL and about -3.5 °C for Y02. This was in good agreement with the calculated radiance offsets above and the two evaluation methods support each other.

#### 2.6.4 Weather data

Weather data is available for both the measurement periods. For the first period the recordings started 24 h before the radiance measurements and for the second period the recordings started 40 h in advance. Some of the results are shown in Appendix 1 and Appendix 2.

During the 8<sup>th</sup> the sky was clear and the weather sunny. The 9<sup>th</sup> the sky was cloudy and at about 13:00 it started to rain mixed with snow. Soon after that the experiment was stopped. When the experiments started again on the 13<sup>th</sup> the ground was partially covered with snow. This lasted for the second measurement period. No precipitation was registered during the second period.

#### 2.6.5 Contact temperatures

The logged contact temperatures are shown in Figure 13 and Figure 14. A fourth probe was placed in the grass between the panel stands. The graphs clearly show the diurnal variations in temperature. The panels reached a considerable temperature on the 8 April even though they were only heated by the sun. The 9<sup>th</sup> was cloudy and not clear as the 8<sup>th</sup> and this resulted in a much lower afternoon temperature. For the 13 and 14 April the panels were heated and the temperature was higher during the entire period. For both cases the panel with low emissive foil showed higher temperatures than the painted panel. The reason is that the heat loss through radiation is lower for a low emissive surface compared to a high emissive one.

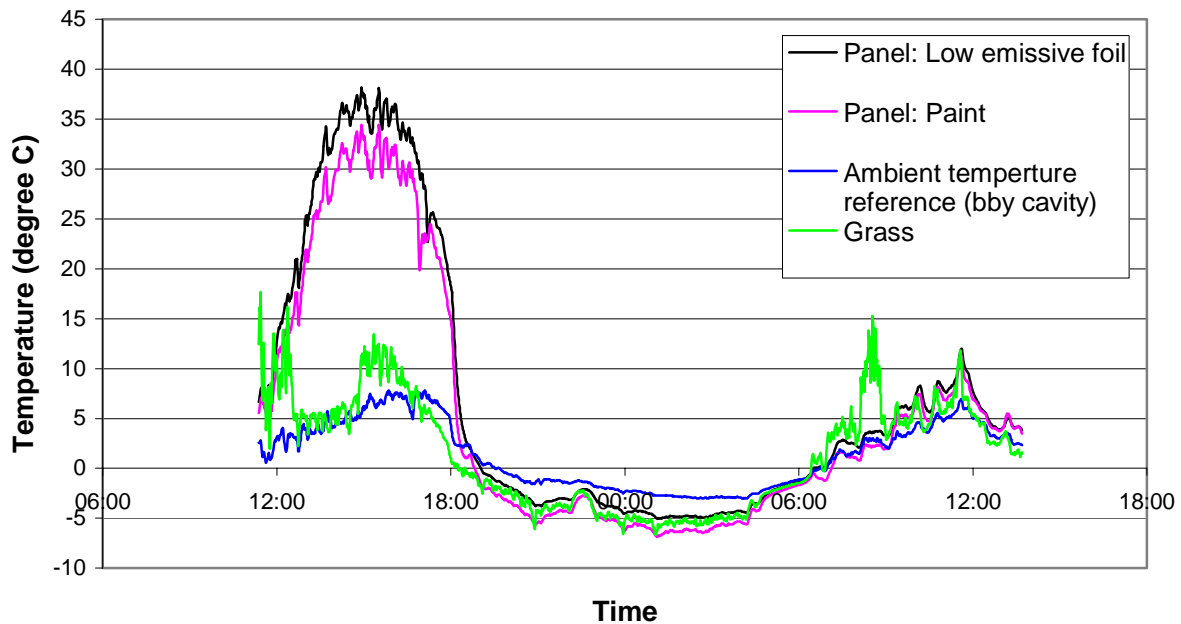


**Figure 13 Contact temperatures for 8-9 April.**

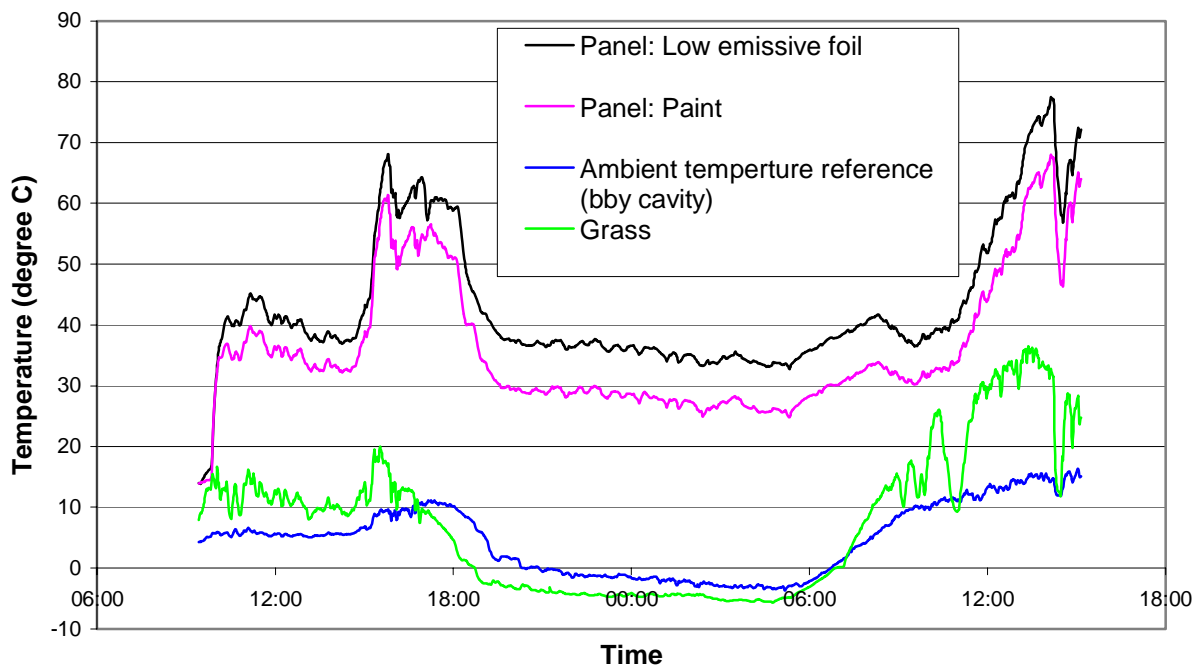


**Figure 14 Contact temperatures for 13-14 April.**

### 3 SIMULATION SOFTWARE

#### 3.1 SENSORVISION

SensorVision, Ref 13 and Ref 17, is a commercial software package used in conjunction with Vega, a 3-D visualisation software package, to simulate infrared (IR) scenes in **real time**. Vega/SensorVision has been developed by Multigen Paradigm Inc. Different versions of the program are available on PC/Windows and Silicon Graphics/IRIX platforms.

SensorVision consists of a main module (sv) which performs the IR radiometric calculations and which is run in conjunction with Vega to render real time IR scenes. SensorVision also consist of the database construction tools referred to as the texture material mapper (tmm) and the MOSART atmospheric tool (mat). The tmm tool is used to assign material properties to the scene (terrain and objects) to produce a database of material codes. The mat tool consists of two subprograms, MOSART and TERTEM, and is used to generate a run time database for atmospheric quantities (MOSART) and surface temperatures (TERTEM). Furthermore, an application programming interface (API) to Vega and SensorVision can be used to create user defined applications.

In SensorVision a simplified radiometric equation is used to calculate the radiance for each pixel in the scene, for a user defined wavelength band and sensor spectral response function. The radiometric equation includes components for incident solar/lunar and sky shine radiance, thermal radiation emitted from the object surface and atmospheric path radiance for the line of sight between the object surface and the sensor. The components in the radiometric calculations are illustrated in Figure 15.

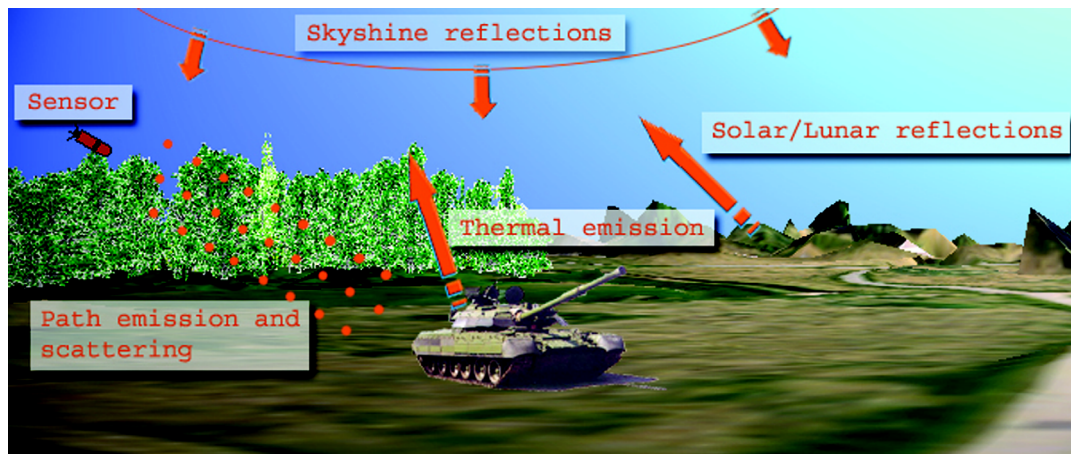


**Figure 15 Schematic illustration of components included in the SensorVision radiometric calculations.**

In SensorVision a number of simplifications and approximations have been used in the implementation of the radiometric equation in order to reach real time performance. Many of these approximations are described in Ref 3. The calculations of surface temperatures, in the mat tool, are performed using a one-dimensional three-layer heat transfer model which includes radiation, convection and evaporation.

The input data to SensorVision consists of for instance material thermal and optical (spectral reflectance) data, textures and triangulated (CAD) models for terrain and objects, weather data and a sensor response function. Output from sensor vision is given as a real time rendered simulation (shown on a computer screen). By using an API, the radiance values calculated by SensorVision can be obtained. However, the radiance values can only be obtained with the same resolution as the pixel bit resolution (see Ref 3).

Some comparisons between simulations using SensorVision and measurements can be found in the literature. Attempts to validate the temperatures calculated with the tool mat have been performed in Ref 4 and Ref 15. A comparison between calculated and measured radiance in the wavelength band 8-12  $\mu\text{m}$  can be found in Ref 1.

### 3.2 CAMEOSIM

Camouflage Electro Optic Simulation System (CAMEO-SIM) is a synthetic scene-generating tool developed by Insys LTD in the UK

Ref 5, Ref 7, Ref 8, Ref 10) over several years and the version (4.2) which was used in this work was released in 2002. CAMEO-SIM (CS) delivers synthetic high fidelity physically based radiance maps of 3D synthetic scenes for a wide range of operational scenarios at wavelengths between 0.4-20  $\mu\text{m}$ . CS requires therefore information on geometry, materials (both thermal, spectral and scattering properties), weather, observer (sensor) etc. CS then uses different (chosen by the user) approximations to solve radiation transport equations (RTE), i.e. providing a range of solutions to the general RTE (

Ref 5). This means that CS is fully scaleable from real-time performance to fully bi-directional radiosity solutions (

Ref 5). There are therefore a number of rendering engines including a recursive importance driven Monte-Carlo ray-tracing algorithm within CS. CS uses MODTRAN4 (version 2) (Ref 12) for setting up the atmospheric environment and consequently to solve the atmospheric RTE. CS is a module based program package and can therefore be easily extended with new considerations (e.g. advanced sensor models, etc) and runs under IRIX or LINUX. In this work a PC-LINUX version of CAMEO-SIM was used.

The atmosphere in CS is divided into a spectral and a thermal atmosphere. MODTRAN4 generate solar/lunar irradiance, path radiance, infinite path radiance, skyshine path radiance and path transmission within the spectral atmosphere. These spectral optical calculations are functions of several and different parameters, e.g. path radiance is a function of solar elevation, observer altitude, solar observer azimuth, Line-of-Sight (LOS) range, and LOS elevation. These MODTRAN4 generated values are normalised for sensor response and observer/facet path transmissivity before entering the ray-tracer algorithms. When generated within the CS-environment a complete 3D atmospheric parameterisation is built up using MODTRAN4.

The thermal atmosphere defines the environmental conditions that dictate the scene's material temperatures, as will be further discussed. In the thermal atmosphere, the following thermal fluxes are modelled: wind, convection, insolation, sky radiation, precipitation, radiation, transpiration, and material conduction (in 1-dimension). The time resolved weather conditions, such as wind speed, air temperature, direct solar radiation etc. are inputs to the thermal atmosphere calculations.

### 3.3 RADTHERM IR

RadTherm, Ref 16, is a cross-platform thermal and infrared signature modelling tool for Windows/UNIX computers which can be used to model the steady state and transient distribution of heat over complex surface descriptions of component systems in a relevant background. RadTherm models 3-D conduction, convection, and multi-bounce radiation and solves the equations using algorithms based on Finite Difference Methods (FDM). A very fast voxel-based ray tracer is used to compute radiation view factors and solar projected (apparent) areas. This ray tracer provides very fast radiation exchange over complex models. The output from RadTherm is the temperature, apparent temperature or the radiance map of the component system which can be analysed and viewed using the integrated post-processor. RadThermIR is written in C++.

Thermal models in RadThermIR are organized into a hierarchical arrangement of nodes, elements, parts and assemblies. Each of them is given specific physical properties. Thermal nodes are the building blocks of RadThermIR models. A thermal node is an isothermal entity for which the RadThermIR solver computes a temperature. Thermal nodes can be represented with or without geometry and the elements are isothermal surfaces that are modeled with geometry. Elements that have the same boundary conditions, thermal and physical properties are grouped into parts. Groups of parts can be further organized in assemblies. RadThermIR includes a large number of wavelength dependent background models, e.g. water, soil, grass or different types of foliage and building structures.

Material properties, e.g. density, heat capacity, heat conductivity and paint or surface properties, and boundary conditions are read from built-in or imported data files, wavelength dependent properties and/or parameter constants. The weather that is influencing the model is imported by text files or modelled by the inbuilt algorithms. Calculated temperature for two sided parts (standard two sided, 3-Layer) will need material properties and boundary conditions for both the front and back sides. Assigned temperature parts and standard insulated parts only require material properties and boundary conditions for the front side.

The models could be equipped with engines and exhaust systems. If so, RadThermIR also calculates the mass flow from the engine through the exhaust system for actual conditions. The engine model uses engine power and engine speed to predict the engine block surface temperature, the exhaust gas temperature, the exhaust gas flow rate and the cooling air temperature, among other properties. Exhaust air and cooling air nodes are automatically created. These nodes can be used in advection networks to simulate the air in the engine compartment as well as gas flow through the exhaust system. The temperature for the engine block will be predicted based on the engine properties only, with the thermostatic temperature specifying the maximum engine block temperature.

The solar algorithms calculate the actual sun position for every time step. The modelled object could be given variable speeds and headings through imported data files. This brings RadThermIR to compute new relative positions for the sun for every time step.

The influence from convection that affects the modelled object could be pre-processed in a CFD-code before analysis in RadThermIR. This option allows the user to import transient convection boundary conditions from a transient convection data file. The fluid film temperatures and convection coefficients from the CFD analysis will be provided for all nodes and all time steps.

All input files and output files are ASCII text files.

## 4 CASE DEFINITIONS AND INPUT DATA

Geometries and designs of the panels were presented in Section 2.1. In this section we briefly present some thermal and optical material data for the panels, which are used as input data to the IR simulations. Software specific input data will be presented in Section 5.

An important quantity in radiometric models is the spectral reflectance. Some models and software also have the ability to treat an angular dependence in the reflectance, through a bi-directional reflectance distribution function (BRDF) for instance. In the simulations presented in this report the panel surfaces are assumed to be diffuse and therefore no angular dependence (or specular reflection) is considered. The reflectance of the two considered panel coatings has been measured at visual and IR wavelengths. At IR wavelengths Hemispherical Directional Reflectance (HDR) data are available and the HDR for 8° incidence angle was used as an estimate for the spectral reflectance used in the simulations.

Thermal material data, which are used in the simulations, are presented in Table 5. The solar absorptivity was calculated from measured reflectance data at the visual wavelengths, weighted against the solar spectral irradiance at sea level (for 1 air mass), Ref 18. The thermal emissivity was estimated from the measured Hemispherical Directional Reflectance (HDR) data. The data for specific heat, conductivity and density for aluminium have been taken from Ref 11 and the data for Divinycell are data provided by the manufacturer in Ref 2. No effort has been made to find accurate values of the characteristic lengths, which is a parameter in thermal convection models, and these values should be seen as very rough estimates.

**Table 5 Thermal material parameters used as common input data in the simulations**

	<b>Paint</b>	<b>Foil</b>	<b>Aluminium</b>	<b>Divinycell</b>
Solar absorptivity	0.805	0.7		
Thermal emissivity	0.8	0.4		
Characteristic length	1 m	1 m		
Specific heat			0.884 kJ/kg/K	1.9 kJ/kg/K
Conductivity			201.073 W/m/K	0.03W/m/K
Density			2770.09 kg/m <sup>3</sup>	48 kg/m <sup>3</sup>

## 5 SIMULATIONS

### 5.1 SENSORVISION

The spectral reflectivity used as input to the SensorVision simulations was taken for HDR measurements with incident light at 8° to the surface normal (see Section 4). In SensorVision the spectral reflectance is used in the calculation of emitted and reflected radiance from the panels.



In SensorVision the maximum number of layers, which can be modelled in the 1D thermal model (in the tool MAT) is three. For the uppermost layer (the surface layer) the user can provide layer thickness and thermal material data such as solar absorptivity, thermal emissivity, conductivity and specific heat as input. The materials for the two sublayers have to be chosen amongst a number of hard coded default materials. Attempts to model the paint coating as an individual layer gave unrealistic results. The conclusion was that SensorVision could not handle such thin layers as the paint coating. The surface layer was therefore given a thickness of 0.004 m with solar absorptivity, thermal emissivity and characteristic length according to Table 5 for paint coating and bulk thermal material parameters as for Aluminium, also in Table 5. The SensorVision default material “insulation”, with a thickness of 0.04 m, was used as the first sublayer instead of Divinycell. For the bottommost layer, the default material “still air” was chosen, see Figure 16.

In the case of the panel with foil, the foil consists of plastic, metal and glass fibre fabric and the thickness is only 0.4 - 0.5 mm so, as for the paint panel, the foil has not been modelled as an individual layer. A surface layer with thickness 0.004 meter was chosen, with solar absorptivity and thermal emissivity for the foil according to Table 5, and bulk thermal material parameters were chosen as for Aluminium, see Table 5. The characteristic length was in this case set to 0.1 m (which is not in accordance with Table 5). For sublayer 1, default material “insulation” with thickness 0.04 meter was chosen and as sublayer 2, default material “Still Air” was set.

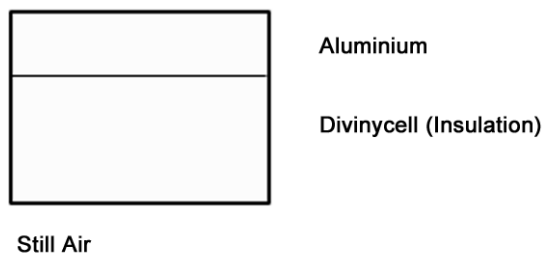


**Figure 16** The structure of layers on the panels

The global position of the panels in the simulation was latitude 58° and longitude 15°. The geometric models of the panels, which have been created in the Multigen Paradigm Inc. OpenFlight format, were the only objects in the SensorVision IR scene simulation. This means that no terrain background was included. The “background” instead only consisted of the SensorVision simulation of sky and atmosphere, which in SensorVision is modelled as isotropic. The motivation for not including a terrain background in the simulations was that SensorVision does not account for thermal and radiometric interaction between objects, such as the panel, and the terrain background.

In the thermal and atmospheric calculations performed in the SensorVision tool MAT, the Fixed Temperature Calibration Point parameter was used. This means that certain weather parameters for one point in time are set. This is the only way available to include measured weather data in SensorVision simulations. We did computations where the fixed temperature calibration point was set at 15.00 and 01.00. At 15.00 the wind speed was 4.3 m/sec, the visibility range 6.47 and surface air temperature was 276 K. At 01.00 the wind speed was 2 m/sec, the visibility range 6.54 and surface air temperature 270 K. The MAT (MOSART) model atmosphere was chosen to be “Sub arctic Winter”, the cloud cover to set to “clear” and

the humidity to “dry”. Response functions (LPL and Y02 from the Thermovision system) were used to simulate the measured LWIR and MWIR spectral bands.

## 5.2 CAMEOSIM

In this work CS has been set up using the weather history measured during the panel measurement campaign 7/4-03 to 9/4-03, see Appendix 1. The weather history used for CS includes direct solar radiation, air temperature, wind speed, and humidity (no rain was included). The input for CS concerning direct solar radiation should not include diffuse scattered sun radiation as this is simulated within the CS environment using MODTRAN 4 (version 2) (Ref 12). Therefore, a slight overestimation of direct solar radiation is probable since the weather station only provided total solar irradiance (direct + diffuse). Furthermore, the convection model includes characteristic length and wind speed. In this case a characteristic length of 1 m was used, but it is likely that a somewhat shorter characteristic length is more accurate. On the other hand, the wind speed used was the one measured from the weather station, which also measures direction. Since the wind direction is not an input parameter in CS, and since the wind was coming obliquely from behind during the 8<sup>th</sup> of April (around 14.00 UTC), one could argue that the wind speed should be decreased at least during this time period. Atmospheric RTE was solved using MODTRAN 4 (Ref 12), which is a module included in CS. MODTRAN was set up to use sub-arctic winter, spring, no cloud, surface of decayed grass, MIE-scattering, and rural visibility (around 6 km for all times).

For the painted panel, the input to CS was a 1 m x 1.22 m geometry with three layers, 4 mm Al, 40 mm Diviny-cell and 4 mm Al. The same layer configuration was used for the foil-covered panel. As CS uses a 1D-thermal solution no lateral considerations were employed. The paint for the painted panel was applied by setting up a perfectly diffuse (no information about the BRDF of the panel surface was known) with the spectral reflectivity (HDR) for 2.0  $\mu\text{m}$  – 25  $\mu\text{m}$ . The foil was treated in the same way without taking the thickness of it into account. The solar absorptivity and thermal emissivity for the painted and the foil-covered panel were chosen in accordance with Table 5. The terrain was set-up in CS as a 3-layer structure. A procedural texture of grass and sand (500 x 500 m<sup>2</sup>) was created to model the ground. Beneath this, a layer of 50 m of soil was assumed and finally at the bottom a 500 m rock as a 10°C heat reservoir.

Both the response functions (LPL and Y02 from the Thermovision system) were used to simulate in LWIR and MWIR, as well as unity LWIR and MWIR response functions for the bands 8-12  $\mu\text{m}$  and 3-5  $\mu\text{m}$ . The latter was introduced to enable comparisons to the RadTherm IR result (see Section 5.3), and the former to model the measuring system Thermovision (see Section 2.4).

Simulations were done in two parts (this is how it has to be setup in CS), one for 24 h for the 8<sup>th</sup> of April, and one for the first 14 hours for the 9<sup>th</sup> of April, Swedish Local Time. The time resolution was set to 15 min for rendering, and 1 min for weather data. The rendering sensor was set to view a set of pixels in the centre of the panels, and using a 1 x 1 pixel resolution (to ease up analysis) sensor. Typically, for a 24-hour time period, a simulation takes about 30 min, with full radiosity, and with a super-sampling of each pixel. This latter is the normal Monte-Carlo sampling used within CS for rendering images with a high resolution. There are several other methods of sampling to increase the statistics of a CS simulation, but as the object is not complex the chosen method is more than enough. That is, differences between

measured data and CS simulation results will not be a result of statistics, more likely a result of approximations such as panel parameters, weather consideration, and the spectral reflectivity employed.

### 5.3 RADTHERM IR

The overall model consists of two parts, the panel and the background that the panel is placed on. The panel is modelled as a 3-layer structure with an additional paint layer on the top and with the dimensions 1m\*1.2m and with 20\*25 elements modelled with a 30 degree angle and the heading of its normal pointing at 256 deg. The background is a horizontal surface that consists of a 5m\*5m area with 50\*50 elements modelled as a foliage background with short grass and with the initial core temperature set to 5°C. This gives approx. 51000 thermal nodes in 2980 elements which all have to be calculated through the simulation period. The material properties used in both models are shown in Table 6 and the parameters for the surface layers in Table 7. The emissivity value on the backside of the panels was set to 0.22.

**Table 6 Material properties**

	<b>Front layer</b>	<b>Middle layer</b>	<b>Back layer</b>
Material	Aluminum	Heat Foil	Divinycell
Thickness (mm)	3	0.5	40
Density (kg/m <sup>3</sup> )	2770	2000	48
Conductivity (W/m K)	201	5	0.024
Spec. Heat (J/Kg K)	884	1000	1900

**Table 7 Surface layers**

	<b>Solar Absorbptivity</b>	<b>Thermal Emissivity</b>	<b>Fresnel Coefficient</b>	<b>Specular Lobe Width</b>	<b>Thermal Conductance (W/cm<sup>2</sup> K)</b>
Paint	0.805	0.80	0	0.15	1e <sup>-7</sup>
Folie	0.70	0.40	0	0.15	1e <sup>-7</sup>
Grass	0.562	0.938	0.01	0.248	4e <sup>-6</sup>

The chosen algorithm for convection was calculated directly by McAdam's plate model. This model is a mixture of natural and forced convection and it also takes the projected area, due to different wind directions, into account. The used formula for the convection coefficient is a linear approach. The formula could be written:  $h = c_1 + c_2 \cdot v$  where  $v$  = wind speed,  $c_1 = 5.7$  and  $c_2 = 3.8$ .

The global position of the model is latitude 58.235 deg. and longitude -15.345 deg. The time zone is -1 hour according to GMT. Furthermore the model is positioned on an altitude of 75 m above the sea level.

The weather parameters collected, once per minute, by the weather station were used as boundaries during the simulations. The different boundary parameters used were: Swedish normal time, Air temperature, Solar irradiation, Wind speed, Humidity, Cloud coverage (set to 0), Sky irradiation (modelled), Wind direction, Rain rate (set to 0).

The simulations were carried out during 37 hours between 00:00 2003-04-08 to 13:00 2003-04-09 with the time step set to 5 minutes. The resulting parameters from the simulation were physical and apparent temperatures, and the radiance in the radiance bands 3-5 and 8-12 micrometers, in all nodes for all time steps. The number of calculated view factors and reflected rays per element were set to an average level.

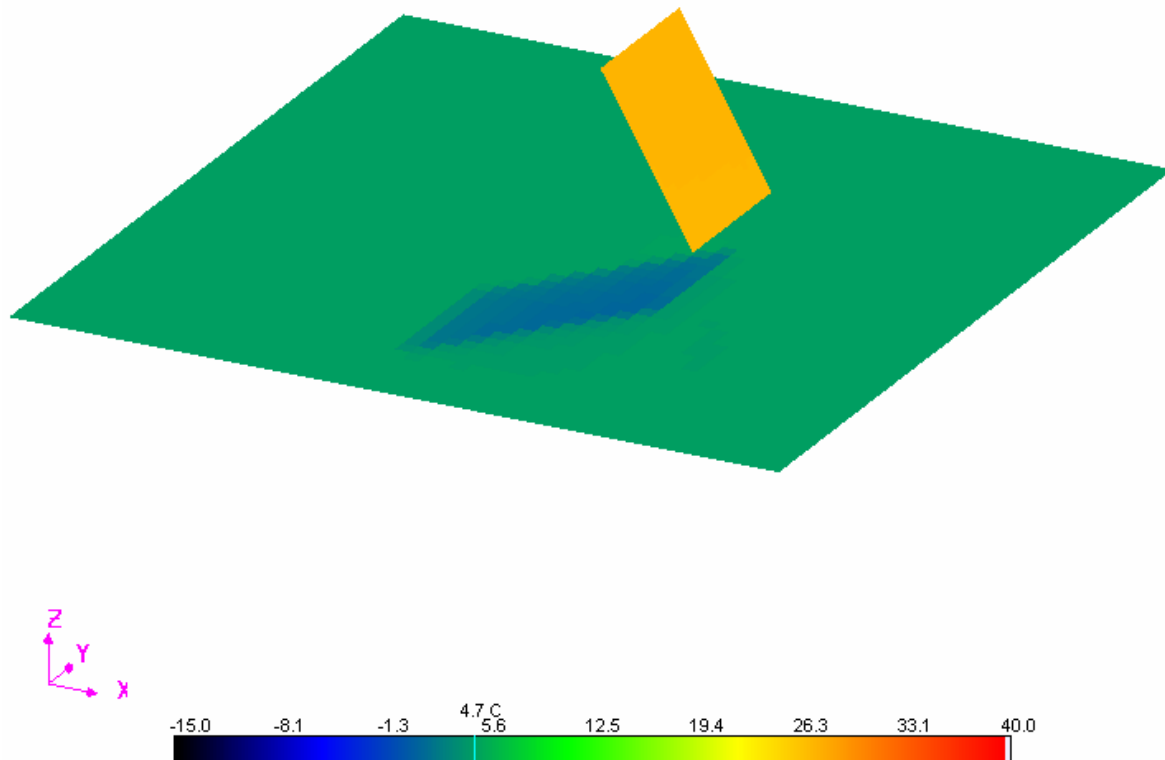


**Figure 17. The RadThermIR model. Also note the dynamic shadow behind the panel.**

A complete simulation for one case took approximately 2.5 hours, after some refinements of the used convergence parameters, on a computer with two P4 2.0 GHz processors and 2 GB SDRAM memory.

## 6 RESULTS

In Chapter 4 and 5 we briefly described input data and how the simulations were performed with the three simulation programs. In this chapter we present results from simulations of the two panels. The results are presented in terms of plots of calculated radiance or surface temperature versus time. The corresponding measured quantities are also included in the plots for comparison. The results will be analysed and discussed in Chapter 7.

## 6.1 SENSORVISION

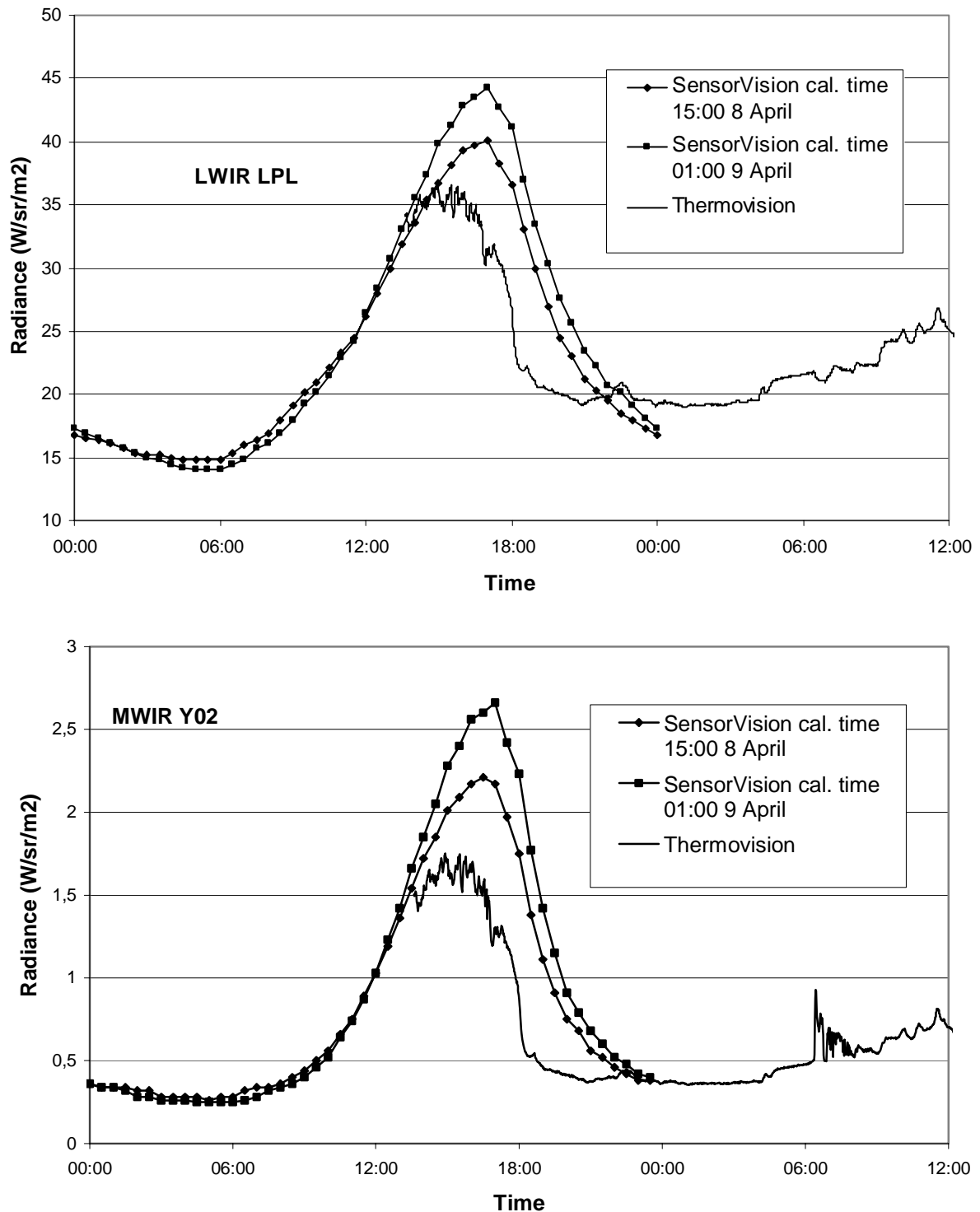


**Figure 18 Comparisons of SensorVision simulations and measurement results from Thermovision for the paint panel in the two wave bands. The SensorVision atmospheric model was calibrated at two different points of time.**

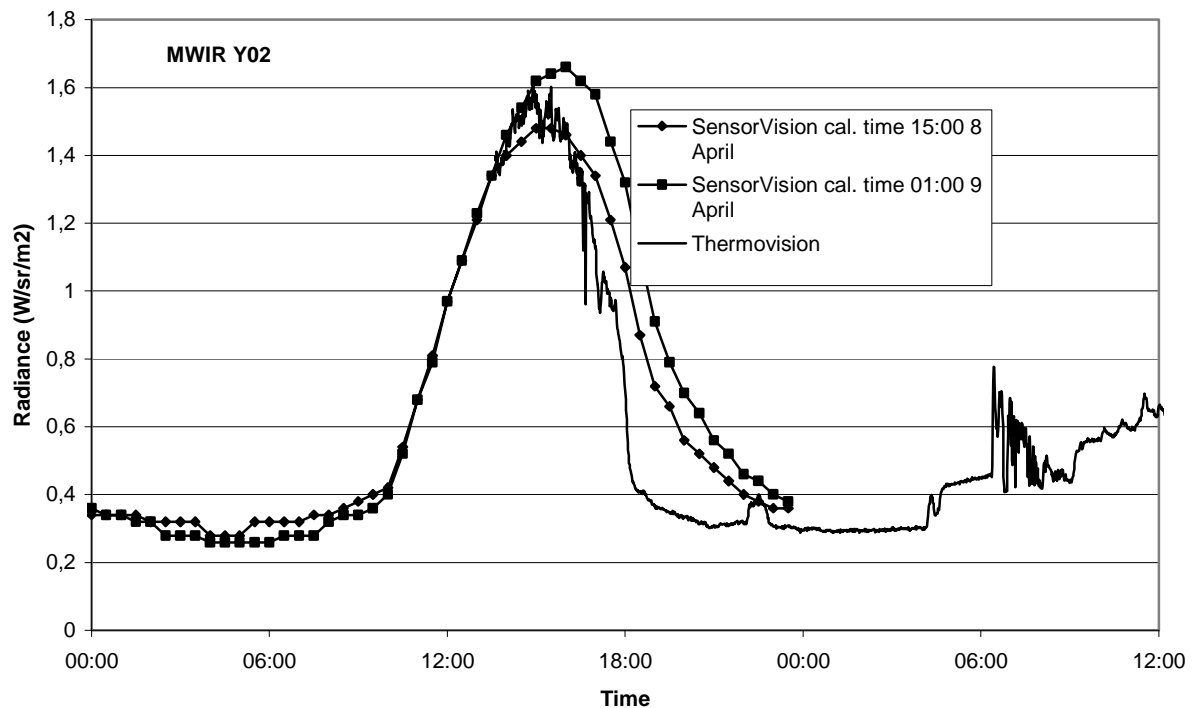
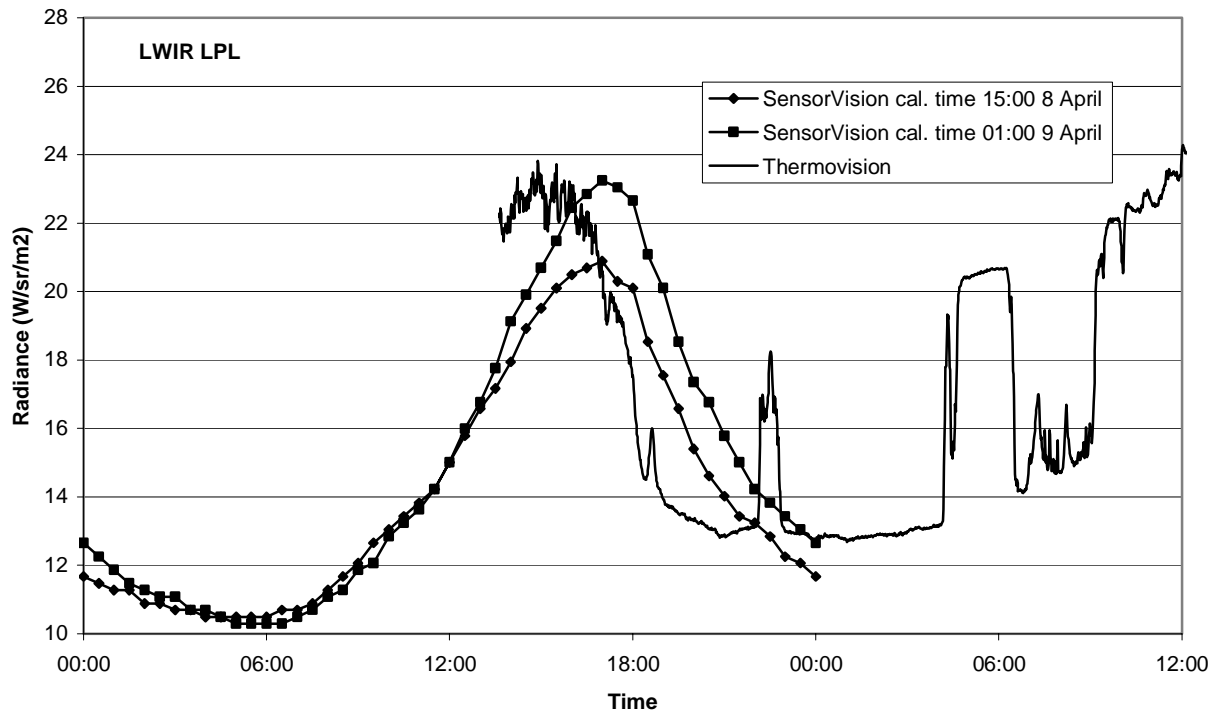


**Figure 19 Comparison of SensorVision simulations and measurement results from Thermovision for the foil panel in the two wave bands. The SensorVision atmospheric model was calibrated at two different points of time.**

## 6.2 CAMEOSIM

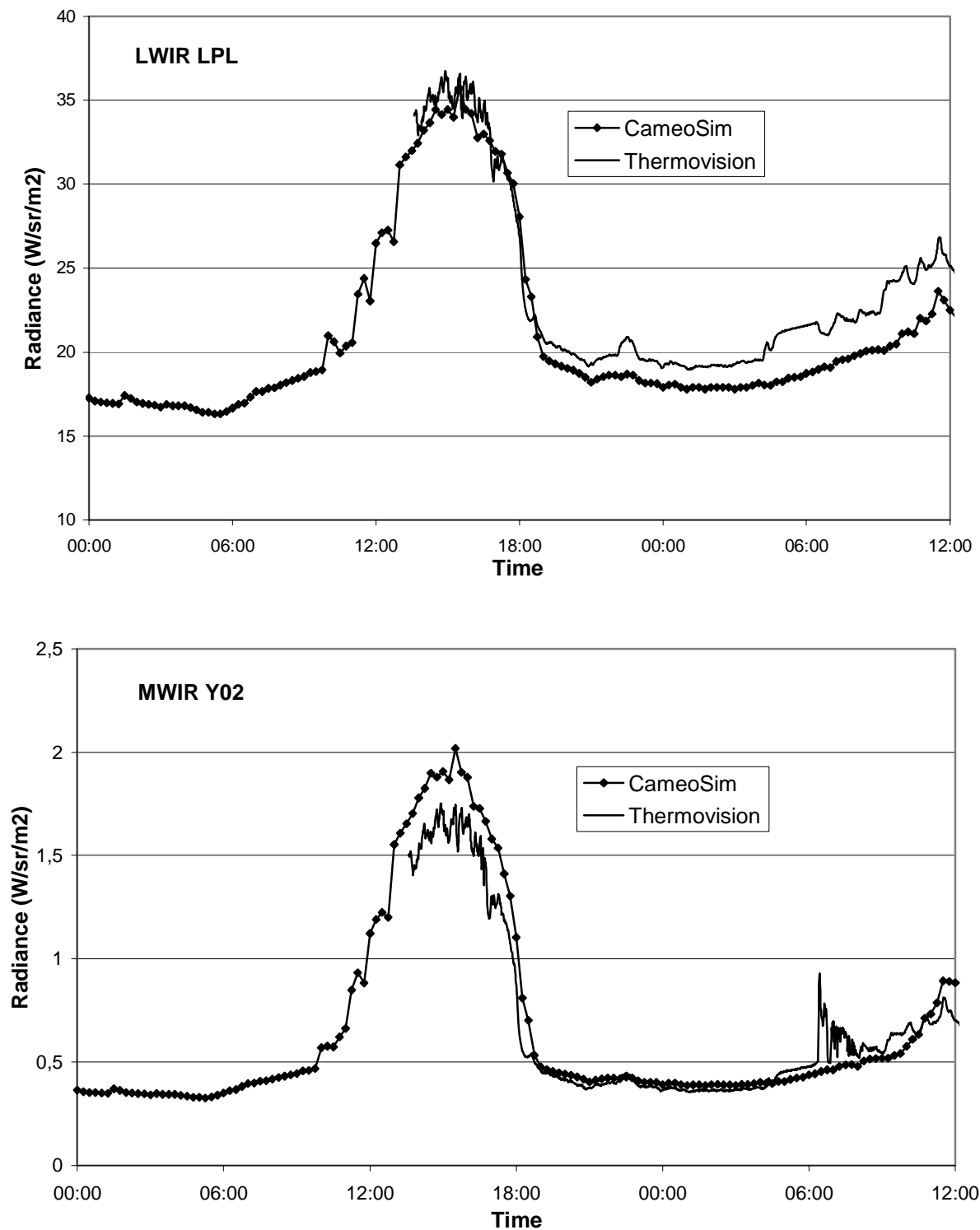


**Figure 20 Comparisons of CameoSim simulations and measurement results from Thermovision for the paint panel in the two wave bands.**

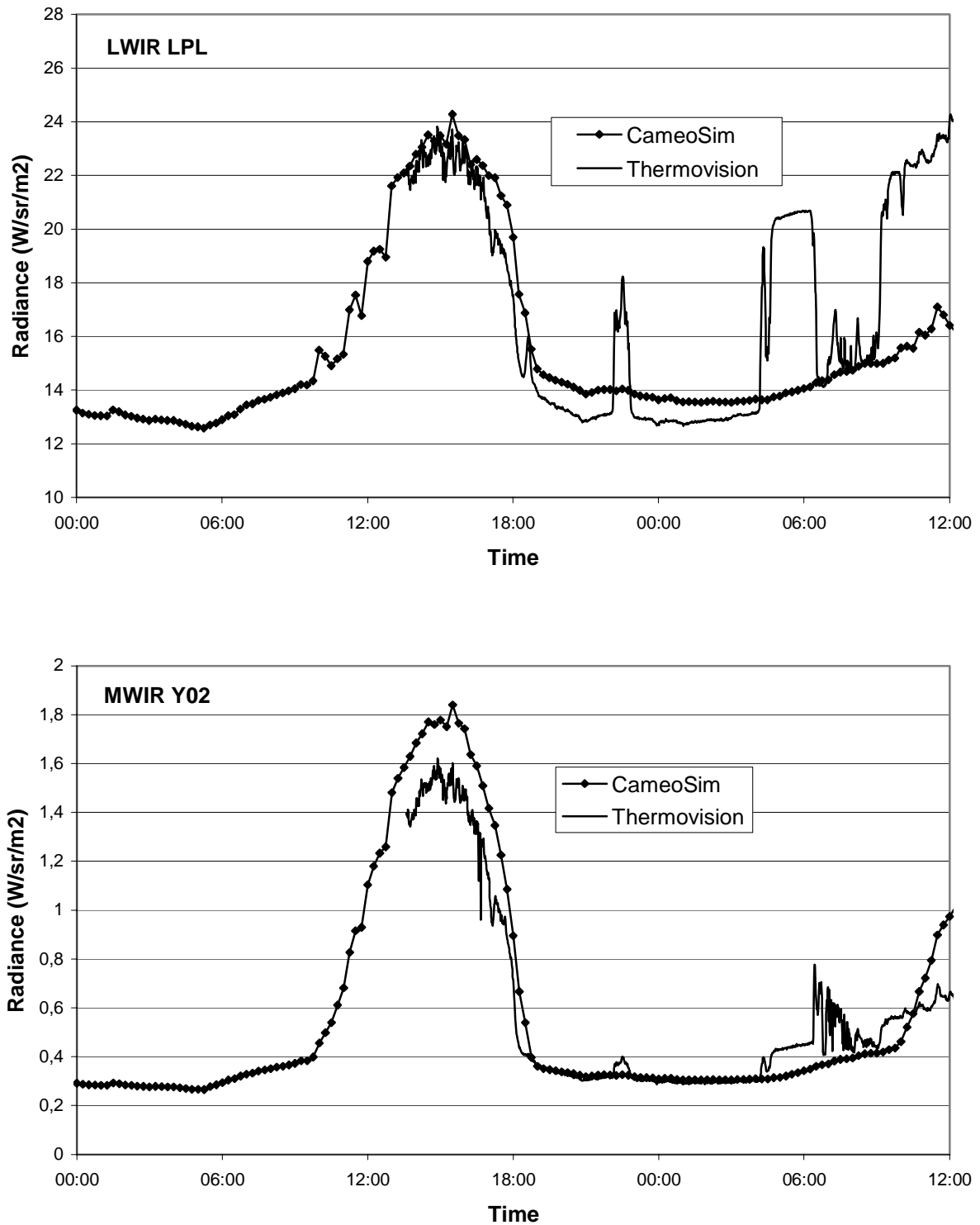


**Figure 21 Comparison of CameoSim simulations and measurement results from Thermovision for the foil panel in the MWIR Y02 wave band.**



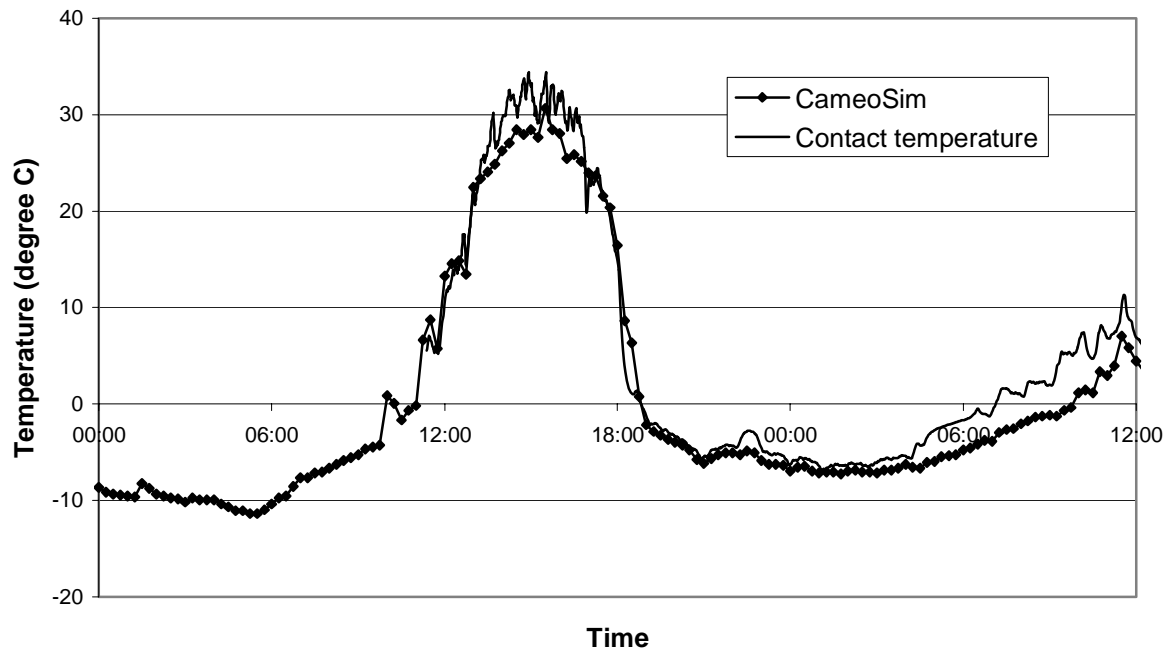


**Figure 22** Comparison of CameoSim predictions of surface temperatures and measured contact temperatures for the paint panel.

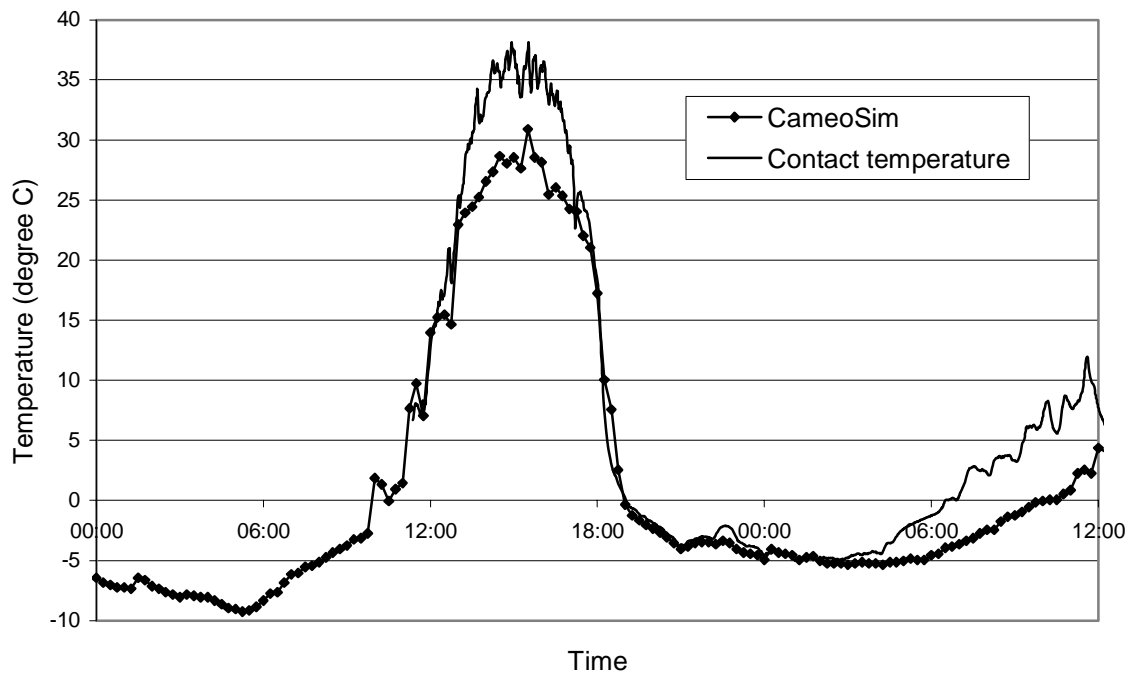


**Figure 23** Comparison of CameoSim predictions of surface temperatures and measured contact temperatures for the foil panel.

## 6.3 RADTHERM IR

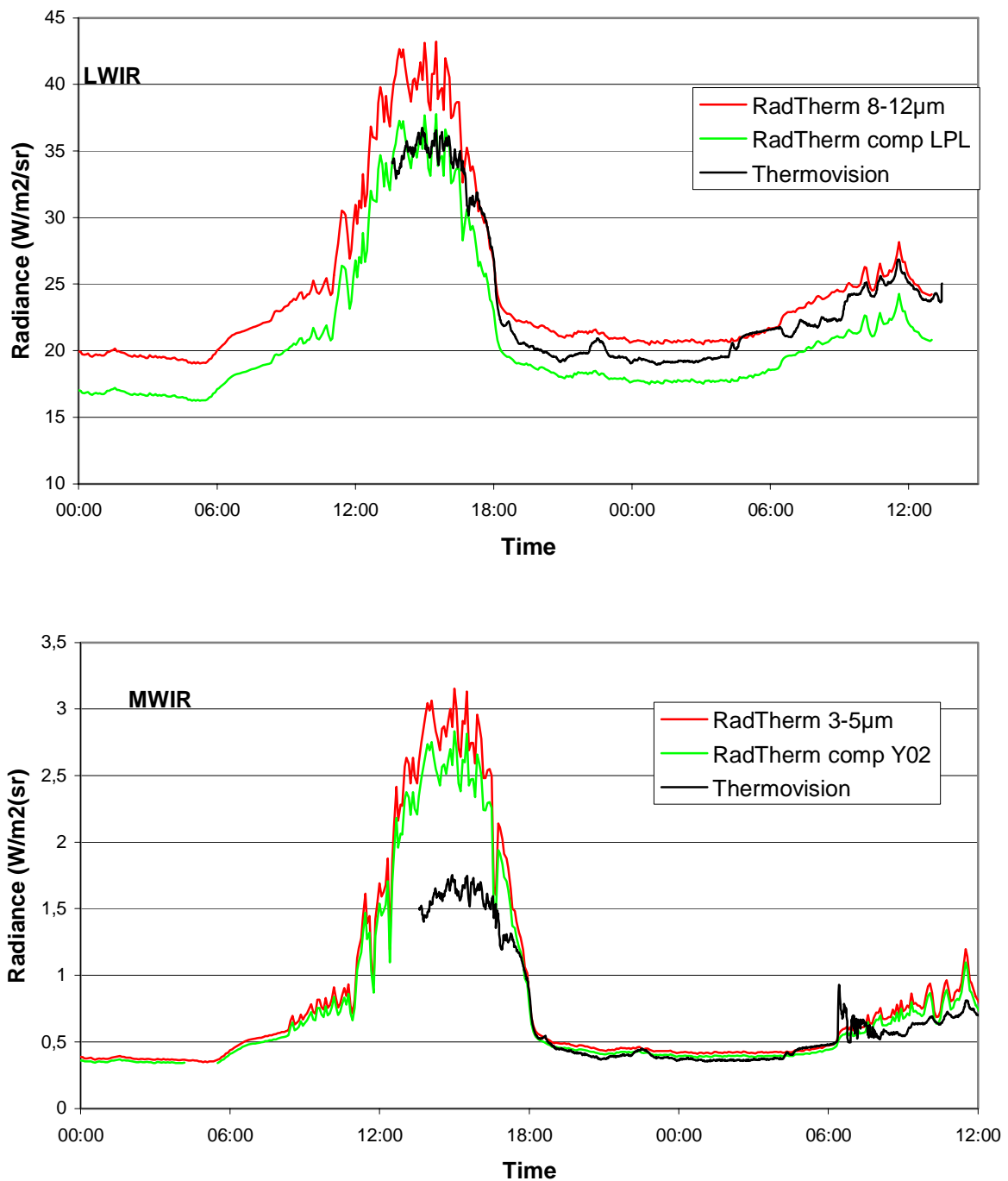


**Figure 24 Comparisons of RadThermIR simulations and measurement results from Thermovision for the paint panel in the two wave bands. Also shown in the diagram is a compensation of the RadThermIR results to yield an LPL or Y02 equivalent radiance. (Assumes that the panel acts as a blackbody)**

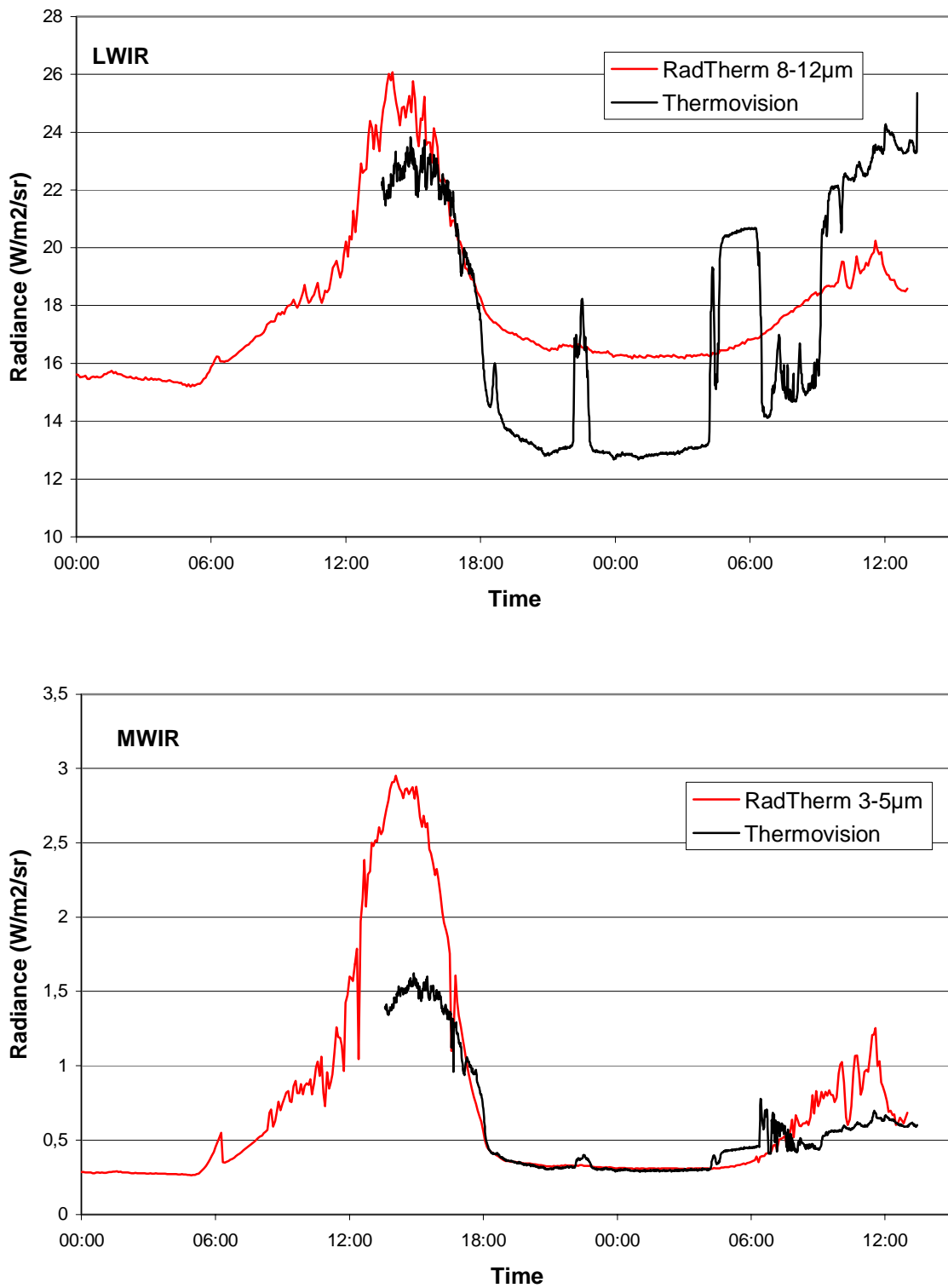


**Figure 25 Comparisons of RadThermIR simulations and measurement results from Thermovision for the foil panel in the two wave bands.**

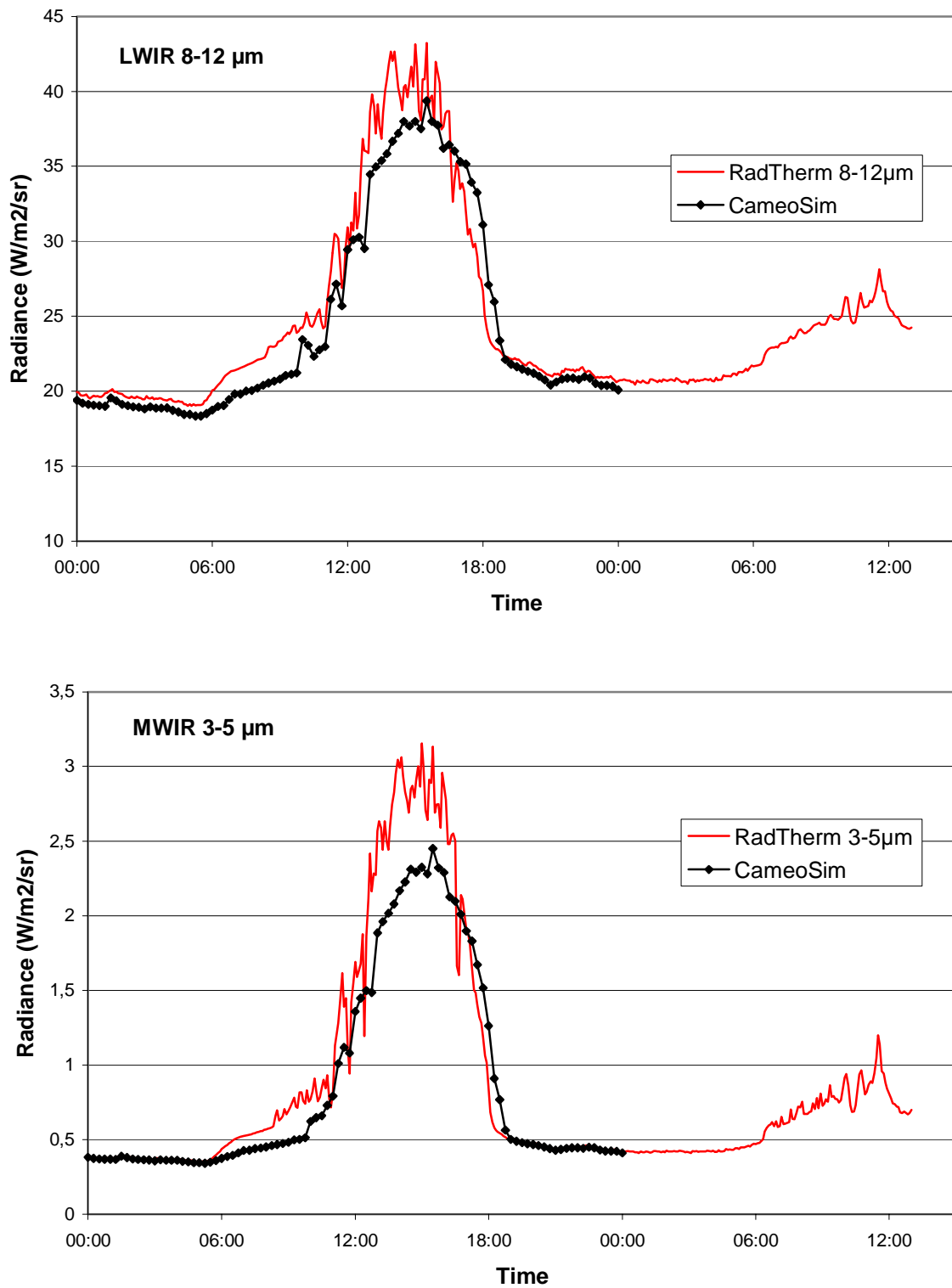


**Figure 26 Comparisons of RadThermIR simulations and CameoSim simulations for the paint panel in the two wave bands. The respons function is set to unity for 3-5 μm and 8-12 μm.**

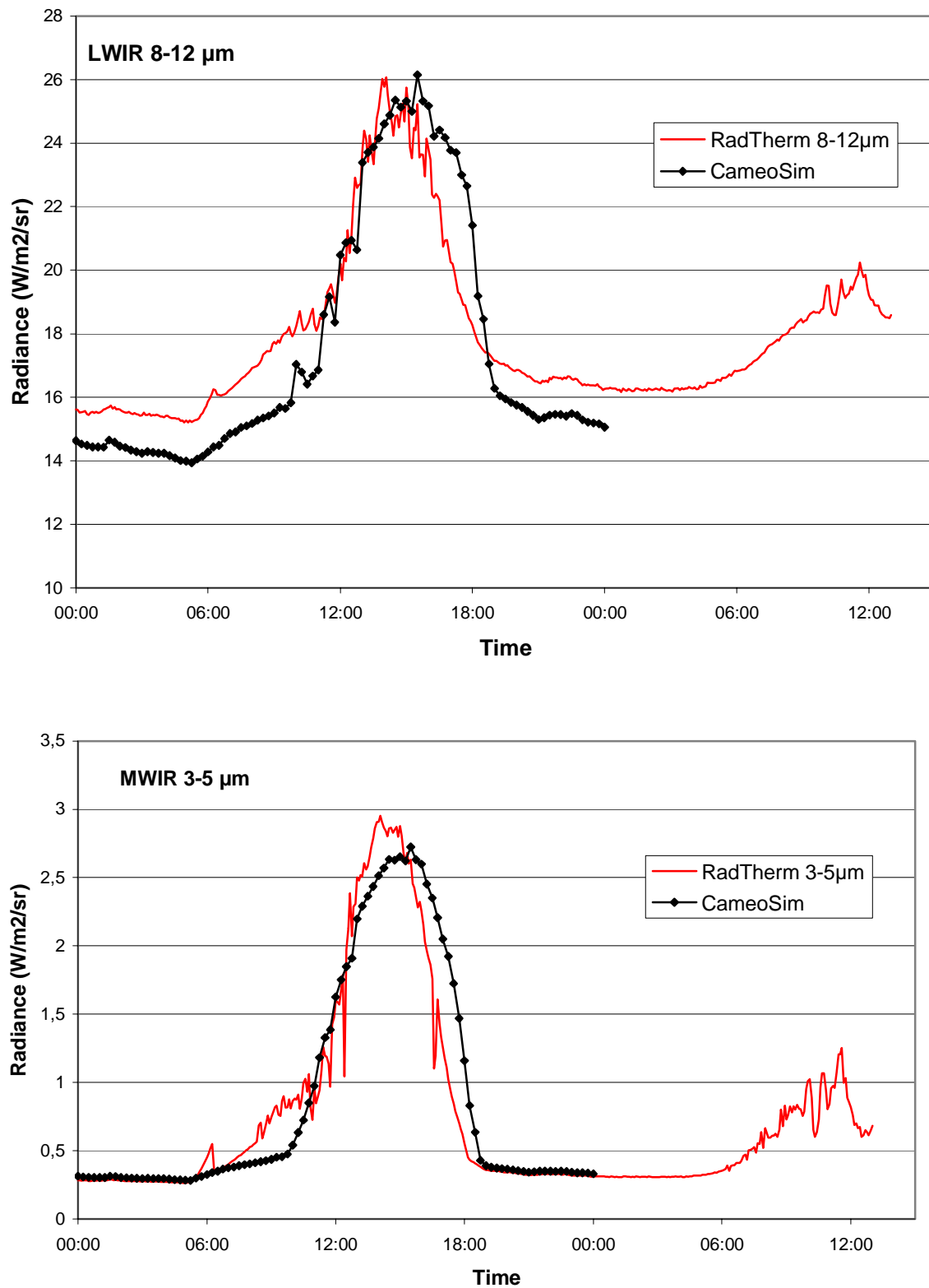


**Figure 27 Comparisons of RadThermIR simulations and CameoSim simulations for the foil panel in the two wave bands. The respons function is set to unity for 3-5  $\mu\text{m}$  and 8-12  $\mu\text{m}$ .**

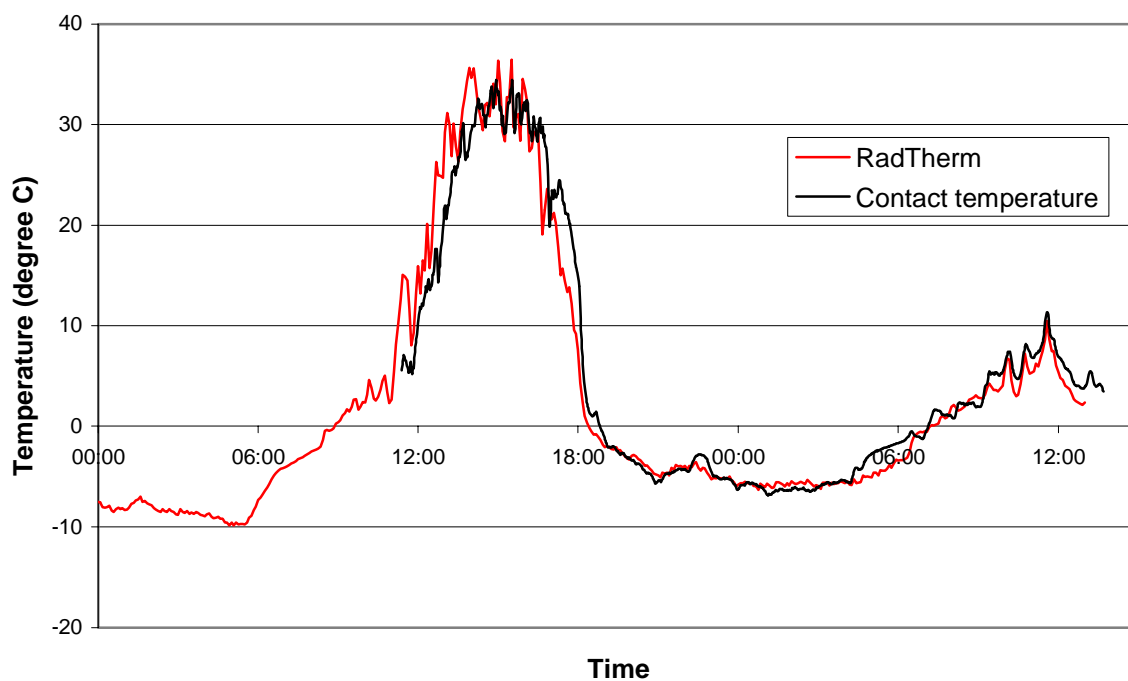


**Figure 28 Comparison of RadThermIR predictions of surface temperature and measured contact temperatures for the paint panel.**

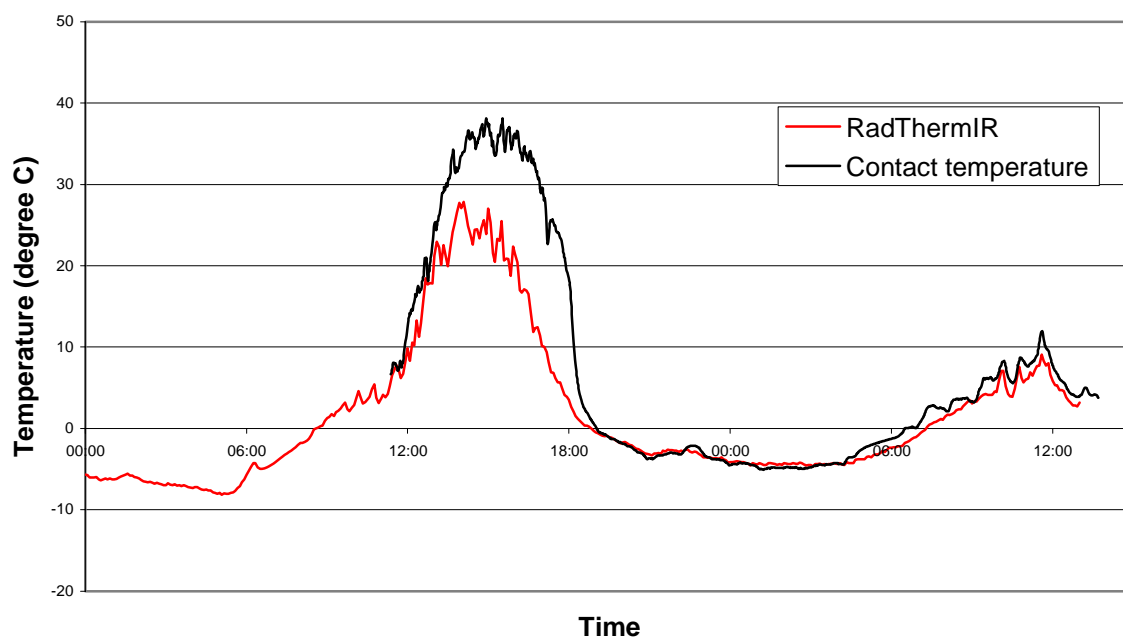


**Figure 29 Comparison of RadThermIR predictions of surface temperature and measured contact temperatures for the foil panel.**

## 7 DISCUSSION

From the plots presented in Section 6 we see that the accuracy of the predictions is varying and seem to be dependent on a number of factors. For instance, the accuracy varies between the three programs, the wavelength bands, the two panels and the time of day (including changes in weather). In general, a number of contributions to the discrepancy between measured and predicted values can be identified. Amongst these are errors and uncertainties in input data, errors and simplifications in the implemented models and errors and uncertainties in the measured data (see Section 2.6.3). All of these factors contribute to the discrepancy between measured and predicted values.

In the following sections we will make a few comments on the results obtained with the three simulation programs.

### 7.1 SENSORVISION

As was mentioned in Section 5.1, the SensorVision simulation does not use the full weather data history as input. Only a limited number of input weather data quantities can be set at a particular point in time in the thermal and atmospheric calculations performed in the tool MAT. This implies that the results depend on the choice of weather data calibration point and that the influence fluctuations in weather (for instance variations in wind speed, cloudiness, humidity, etc.) cannot be accounted for, resulting in a very smooth predicted radiance versus time. In Figure 18 and Figure 19 we can compare the results for two choices of calibration times and we see that the choice of calibration time affects the predicted radiance over time.

We notice from Figure 18 and Figure 19 that the measured radiance, in both wavelength bands, is over-predicted in the SensorVision simulations of the paint panel. This over-prediction stems from an over-prediction of surface temperatures in the tool MAT. We also see that there is a lag in time between the calculated radiance and the measured radiance for all simulation cases. For instance, the maximum predicted radiance is reached more than an hour later than the measured maximum radiance. This time lag seem stem from a time lag in the surface temperatures calculated in the tool MAT and no certain explanation for this discrepancy can be given at present.

### 7.2 CAMEOSIM

Results from simulations of the paint and foil panels are shown in Figure 20 to Figure 23 in Section 6.2. Since the known surface temperatures are a prerequisite for calculating the radiance, we first consider the comparison between predicted and measured surface (contact) temperatures shown in Figure 22 for the paint panel and in Figure 23 for the foil panel. We see that the predicted surface temperatures agree quite well with the measured contact temperatures. However, the measured contact temperatures are somewhat underestimated during daytime, something that is most noticeable for the panel with low emissive foil. The reason for this could, at least in part, lie in uncertainties in input data for the material parameters. For instance the values used for solar absorptivity, thermal emissivity and characteristic length are likely to have uncertainties which when combined are large enough to cover the discrepancy.

Deficiencies in the models implemented in CAMEO-SIM of course also contribute to the prediction errors of surface temperatures. For instance, the modelling of convective heat transfer does not account for the details of the airflow around the object and there is no dependence on wind direction in the heat transfer coefficient used in CameoSim.

Another known source of error is, as was mentioned in Section 5.2, the fact that direct solar radiation input to CAMEO-SIM should not include diffuse scattered sun radiation. Furthermore, there was a problem with the sky radiation sensor on the weather station during the measurements. This had the consequence that the measured sky radiation data could not be used as input and the long wave sky radiation was instead calculated by MODTRAN4 in the CAMEO-SIM environment. Since this calculation was performed for clear sky conditions, the effects of clouds are not accounted for in the long wave sky irradiation on the panels.

Considering the comparisons between measured and predicted radiance in Figure 20 - Figure 21, one should keep in mind that the errors in predicted temperatures are propagated, as one out of several sources of error, into the predicted radiance. We see from the figures that the calculated radiance generally agrees quite well with the measured data. The largest discrepancy is found during the second day (April 9) in the LWIR band for the panel with foil coating. As was mentioned in Section 2.6.2, the dramatic shifts in measured LWIR radiance from the foil panel during the night of April 9 is most likely an effect of changing cloudiness. A probable explanation for this discrepancy between calculations and measurements is the fact that the MODTRAN4 calculations in CAMEO-SIM were performed for clear sky conditions and therefore, the effect of varying cloud conditions are not accounted for in the reflected radiation from the panels. Since the panel with foil has a higher reflectance than the paint panel at IR wavelengths the effect is most noticeable for the foil coating.

### 7.3 RADTHERM IR AND COMPARISON WITH CAMEOSIM

In Figure 24 and Figure 25 the predicted radiance is compared to the measured one. RADTHERM IR predicts the radiance in the wave band 3-5  $\mu\text{m}$  and 8-12 $\mu\text{m}$  with unity responsivity. The measured data however, are reported for the Thermovision spectral responses LPL and Y02 seen in Figure 4. Therefore the values are not directly comparable. For the painted panels in Figure 24 a correction is also included, valid for the assumption that the radiation originates from a blackbody. This is of course not completely true but gives a hint of what the correct level could be.

Many of the general comments made concerning the results obtained in the CAMEO-SIM simulations are also valid for the RADTHERM IR simulations. For instance, since the long wave IR sky radiation sensor on the weather station was out of order during the measurements, this component had to be modelled in RadTherm IR. Furthermore, as was the case in the CAMEO-SIM simulations, the radiometric calculations in RadTherm IR were performed for clear sky conditions and therefore the effect of varying cloud conditions are not accounted for in the reflected radiation from the panels. This is most clearly seen in Figure 25 for the panel with foil coating in the LWIR band.

We see from Figure 28 that the measured surface temperature was predicted rather well during most of the simulated period for the paint panel. For the panel with foil coating, on the other hand, the calculated surface temperatures clearly under-predict the measured temperatures during daytime, which is most noticeable April 8. A somewhat similar behaviour could



be seen in the CAMEO-SIM but still it is difficult to conclude with any certainty whether the discrepancy is mainly due to uncertainties and errors in input data or deficiencies in models.

In Figure 26 and Figure 27 we compare the radiances calculated with RadTherm IR to the radiance obtained in the CAMEO-SIM calculations. In this comparison it should be noted that the response functions used in these CAMEO-SIM and Radtherm IR is set to unity for 3-5  $\mu\text{m}$  and 8-12  $\mu\text{m}$  (compare with Figure 24). Since the calculations for the panels have been performed in a similar way in CAMEO-SIM and RadTherm IR, the results obtained with the two programs are expected to agree quite well. From the figures we see that there is a clear correspondence between the results but there are also discrepancies. It is likely that there are many causes for these discrepancies. Differences in models, numerical algorithms and implementations in the two programs are obvious causes for differences in the results.

## 8 CONCLUSION

In this report we have presented results from a measurement campaign as well as results from calculations, using the three IR signature programs SensorVision, CameoSim and RadThermIR. The calculations have been performed so as to simulate measurements of surface temperature and radiance from targets consisting of two panels with quite different surface emissivities. The simulations, using the three programs, have been compared with the measured data and with each other. Input data to the simulations consists of for instance measured spectral reflectance of the panel coatings, thermal material data, geometry, model parameters and measured weather data.

The comparison between measured and calculated radiance show an agreement, which generally can be said to be according to expectations for CAMEO-SIM and RadTherm IR, when considering the uncertainties in input data. In the case of SensorVision there seems to be a time lag between measured and predicted data which we can not explain at present.

We have tried to identify some possible causes for discrepancies between measured and predicted data. Some of the input data used in the simulations have uncertainties (or errors) which are likely to account for part of the discrepancies between measurements and predictions. Deficiencies in the models used in the programs are also likely to contribute to the prediction errors. We have also concluded that in the way the calculations were performed, the effect of changes in cloudiness (and other atmospheric conditions) is not accounted for in the radiation reflected from the panels. This resulted in rather large discrepancies between measured and calculated radiance from the panel with foil coating during times of changing cloud conditions.

The study presented in this report has provided insight and knowledge about the validity of predicting IR signatures using the three programs SensorVision, CAMEO-SIM and RadTherm IR. However, a continued work on validating the programs could give further information on their validity. For instance, it would be useful to perform a validation where the uncertainties in input data are accounted for in the simulations. The simulations could possibly also be performed in such a way that the actual cloud conditions are accounted for in a better way in the radiometric calculations. Validating the programs for other conditions and objects could also be of value.

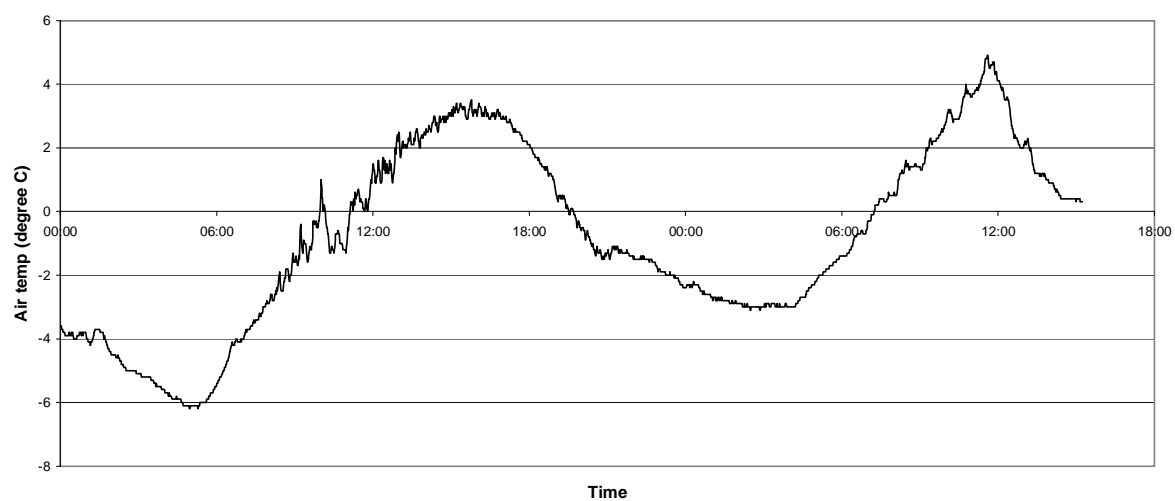
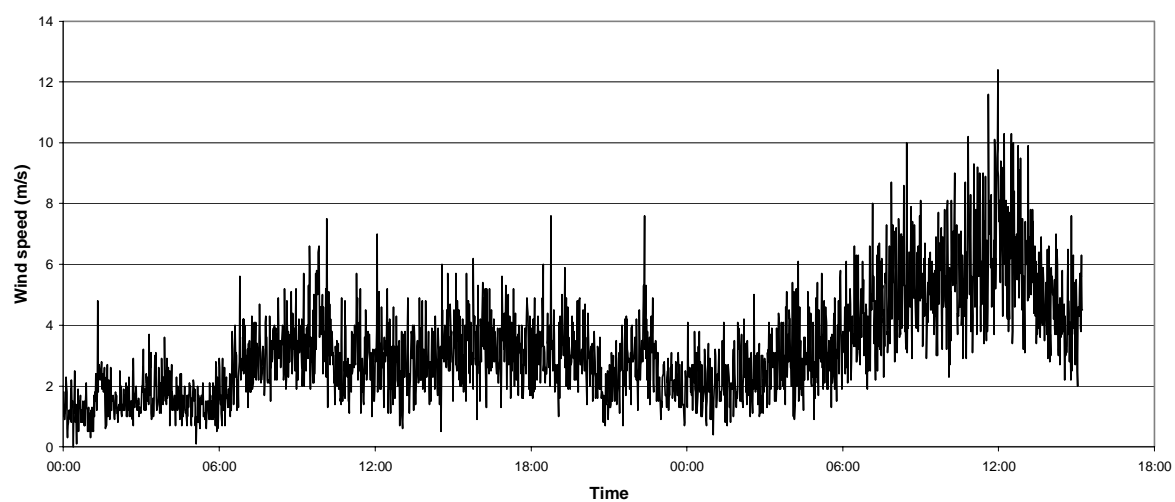
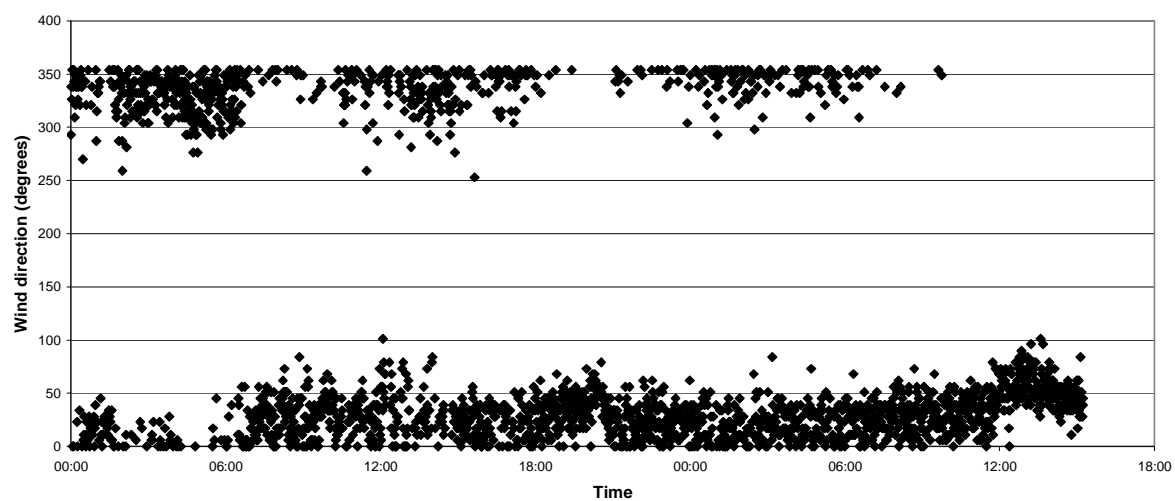
Finally, one of the large benefits of a work like this is that it gives an opportunity to get really acquainted with the programs. They are all complex and require a lot of input data. There are also a considerable amount of settings in the programs that has to be made correctly in order to get reliable results. An exercise like the work presented in this report gives a possibility to use the programs under controlled conditions and to correct imperfections before more challenging simulations are made. The results in this report are encouraging and the programs will be applied to more complex targets and backgrounds.

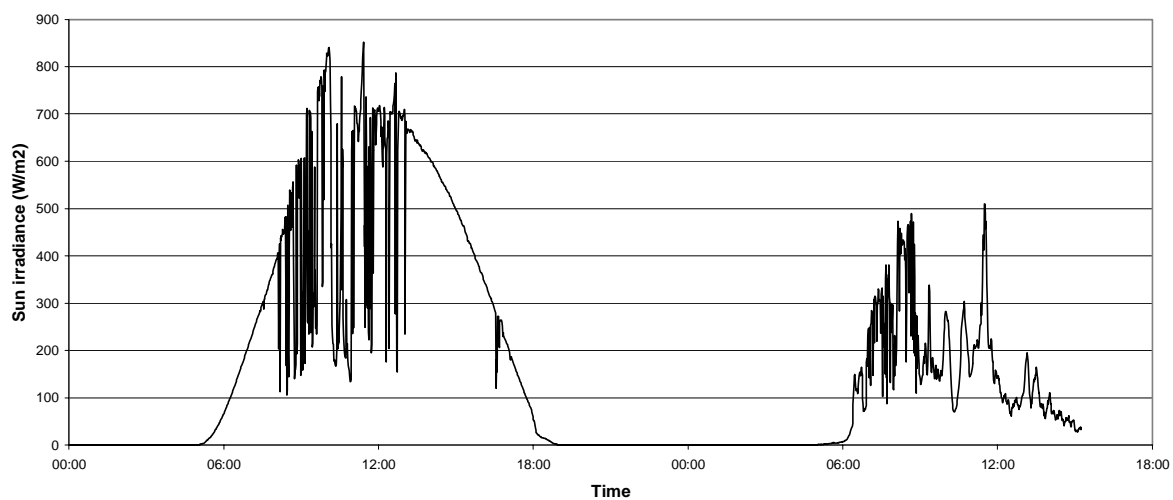
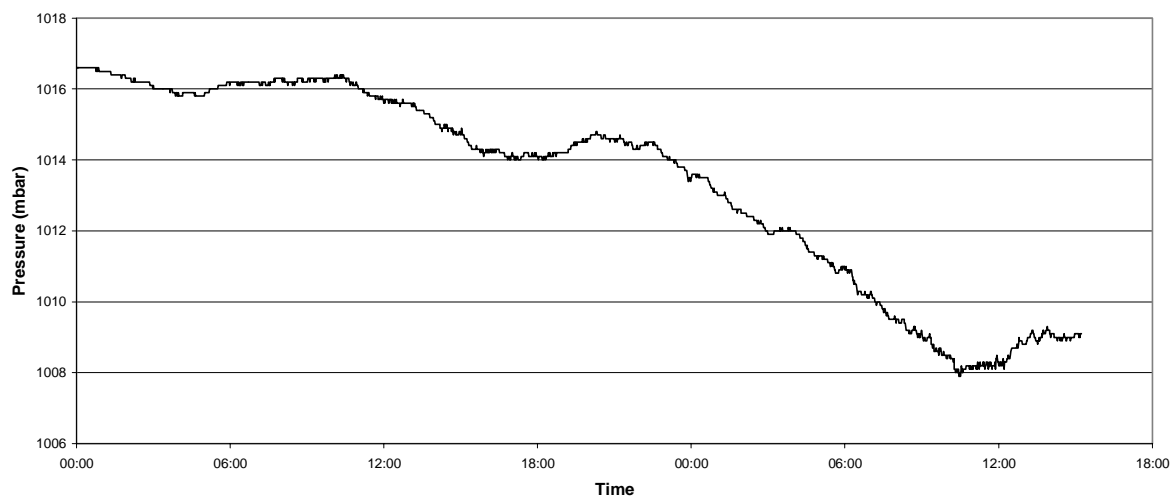
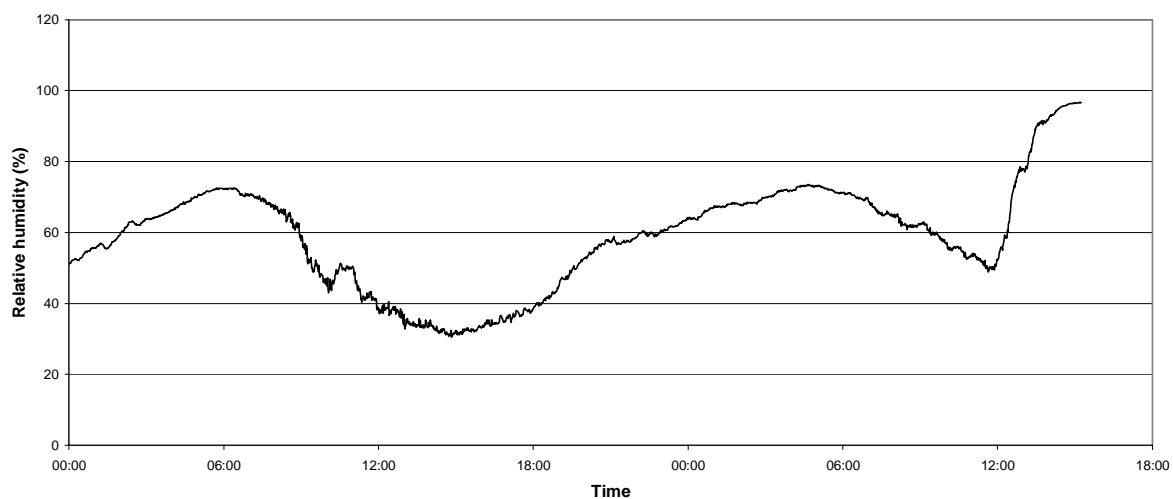
## 9 REFERENCES

- Ref 1** E. Bernardsson, "Initial Validation of SensorVision – A Program for Real-Time IR Simulations", FOI-R--0083--SE, 2001.
- Ref 2** [www.diabgroup.com](http://www.diabgroup.com)
- Ref 3** Duong, N., Wegener, M. 1999, "SensorVision Radiometric Equations (Version 2.2)", DSTO-TN-0193, Defence Science and Technology Organisation, Australia.
- Ref 4** Duong, N., Wegener, M. 2000, "SensorVision validation: diurnal temperature variations in northern Australia", Proc. of SPIE Conf., Technologies for Synthetic Environments: Hardware-in-the-Loop Testing V, vol. 4027.
- Ref 5** D. Filbee et al., "Modeling of High Fidelity Synthetic Imagery for Defence Applications", Proceedings of SPIE, Vol 4718, 2002, p. 12.
- Ref 6** Daniel Fäldt, Johan Ohlsson, Improved infrared object signature calculations for SensorVision by the use of RadTherm, FOI-R--0574--SE
- Ref 7** M.A. Gilmore et al., "Assessments of synthetic image fidelity", Proceedings of SPIE, Vol 4718, 2002, p. 23.
- Ref 8** I.R. Moorehead et al., "CAMEO-SIM: a physics-based broadband scene simulation tool for assessment of camouflage, concealment, and deception methodologies", Optical Engineering, Vol 40, No. 9, Sept 2001, p. 1897.
- Ref 9** C. Nelsson and P. Nilsson, eds., "Measurement Equipment at the Department of IR Systems", FOA-R--99-01111-615--SE, 1999.
- Ref 10** S. Newman et al., "Validation of the use of synthetic imagery for camouflage effectiveness assessment", Proceedings of SPIE, Vol 4718, 2002, p. 35.
- Ref 11** Carl Nordling, Jonny Österman, "Physics Handbook for Science and Engineering", Studentlitteratur, 1980, 1996
- Ref 12** See e.g., [www.ontar.com](http://www.ontar.com) and/or F.X. Kneizys et al., "The MODTRAN 2/3 Report and LOWTRAN Model", Ontar Corporation, 9 Village Way, North Andover, MA 01845, USA, 1996.
- Ref 13** SensorVision Technical Description, Paradigm Simulation Inc., 1998

- Ref 14** Stefan Sjökvist, Mikael Georgsson, "Värmeöverföringsanalys i olika skrovstrukturer", FOA-R--00-01761-615--SE, 2000.
- Ref 15** Special Technical Report: Validation of Sensor Vision, Paradigm Simulation Inc., 1998
- Ref 16** <http://www.thermoanalytics.com/products/index.html>
- Ref 17** Vega Sensors, MultiGen-Paradigm Inc., 1999
- Ref 18** George J. Zissis, Editor, "The Infrared & Electro-Optical Systems Handbook, Sources of Radiation", Volume 1, SPIE OPTICAL ENGINEERING PRESS, 1993

## Appendix 1      Weather data from 8-9 April





## Appendix 2      Weather data from 13-14 April

